Electronic supporting information for

Helical pre-organization of molecules drives solid-state intermolecular acyl-transfer reactivity in crystals: Structures and reactivity studies of solvates of racemic 2,6-di-*O*-(4-fluorobenzoyl)-*myo*-inositol 1,3,5-orthoformate

Shobhana Krishnaswamy*,[a,b] Mysore S. Shashidhar*,[c] Mohan M. Bhadbhade[d]

[a]Center for Materials Characterization, CSIR-National Chemical Laboratory, Pune 411008, India. Fax: 91-20-25902642; Tel: 91-20-25902252; E-mail: cy14ipf04@smail.iitm.ac.in

[b]Present address: Department of Chemistry, Indian Institute of Technology Madras, Chennai 600036, India.

[c]Division of Organic Chemistry, CSIR-National Chemical Laboratory, Pune 411008, India. Fax: 91-20-25902629; Tel: 91-20-25902055; E-mail: ms.shashidhar@ncl.res.in

[d]Mark Wainwright Analytical Center, University of New South Wales, Sydney, Australia. Fax: 61-2-93854663; Tel: 61-2-93859898.E-mail: m.bhadbhade@unsw.edu.au

Table of Contents.

Experimental

General procedure for acylation

Freshly distilled acid chloride was added to a cooled solution of *myo*-inositol 1,3,5-orthoformate in dry pyridine, with constant stirring. The reaction mixture was brought to room temperature, stirred for 18 – 20 h and quenched with ice. Pyridine was removed under reduced pressure by co-evaporation with toluene (3×10 mL) and the residue was diluted with ethyl acetate and washed successively with water, 2% aqueous hydrochloric acid, water, saturated sodium bicarbonate solution and water followed by brine. The organic layer was dried over anhydrous sodium sulfate and the solvent was evaporated under reduced pressure. The residue was flash chromatographed on silica gel by gradient elution with light petroleum - ethyl acetate mixture.

Racemic 2,6-di-*O*-(4-fluorobenzoyl)-*myo*-inositol 1,3,5-orthoformate (**12**) and **2-*O*-(4-fluorobenzoyl)-*myo*-inositol 1,3,5-orthoformate** (**18**).

myo-Inositol 1,3,5-orthoformate (0.760 g, 4 mmol) was acylated as described in the general procedure with 4-fluorobenzoyl chloride (~8.4 mmol) in dry pyridine (12 mL), yielding a golden yellow gum. The products were separated by silica gel column chromatography to obtain racemic **12** (1.104 g, 63%) and **18** (0.150 g, 9%).

Data for **12**:

Mp: 176.5-178.5 ºC;**IR** (Nujol, cm^{-1}) ν: 3446, 1730, 1721; **^{1}H NMR** (200 MHz, CD_3COCD_3): δ3.66-3.72 (1H, m), 3.80-3.97 (3H, m), 4.42 (1H, d, *J* = 4 Hz), 4.89-5.00 (3H, m), 6.47–6.63 (4H, m), 7.34-7.48 (4H, m) ppm;**^{13}C NMR** (50.3 MHz, CD_3COCD_3): δ 65.3, 67.8, 69.7, 69.8, 70.5, 72.9, 103.8, 116.5 (d, $^{2}J_{C\text{-}F}$ = 22 Hz), 127.2 (d, $^{4}J_{C\text{-}F}$ = 3 Hz), 127.4 (d, $^{4}J_{C\text{-}F}$ = 3 Hz), 133.4 (t, $^{3}J_{C\text{-}F}$ = 9 Hz), 164.9, 165.5, 166.8 (d, $^{1}J_{C\text{-}F}$ = 252 Hz) ppm; **^{19}F NMR** (376.5 MHz, $CDCl_3$): -104.8 (1F, s), -104.3 (1F, s), -162.1 (C_6F_6) ppm; **Elemental analysis:** Calcd. for $C_{21}H_{16}O_8F_2$: C, 58.07; H, 3.71. Found: C, 57.81; H, 3.52 %.

Data for **18**:

Mp: 174-176 ºC;**IR** (Nujol, cm^{-1}) ν: 3520-3350, 1704; **^{1}H NMR** (400 MHz, CD_3SOCD_3): δ4.18-4.23 (1H, m), 4.24-4.31 (2H, m), 4.38-4.44 (2H, m), 5.45-6.05 (4H, m), 7.37 (2H, t, *J* = 8 Hz),

8.06-8.14 (2H, m) ppm;**^{13}C NMR** (100.6 MHz, CD_3SOCD_3): δ 64.5, 67.5, 70.0, 72.2, 102.2, 116.5 (d, $^2J_{C\text{-}F}$ = 22 Hz), 126.5 (d, $^4J_{C\text{-}F}$ = 2 Hz), 132.8 (d, $^3J_{C\text{-}F}$ = 9 Hz), 164.7, 165.8 (d, $^1J_{C\text{-}F}$ = 252 Hz) ppm; **^{19}F NMR** (376.5 MHz, CD_3SOCD_3): -106.1 (1F, s), -163.5 (C_6F_6) ppm; **Elemental analysis:** Calcd. for $C_{14}H_{13}O_7F$: C, 53.85; H, 4.20. Found: C, 53.94; H, 4.05 %.

2,4,6-tri-*O*-(4-fluorobenzoyl)-*myo*-inositol 1,3,5-orthoformate (**15**)**.**

myo-Inositol 1,3,5-orthoformate (0.950 g, 5 mmol) was acylated as described in the general procedure with 4-fluorobenzoyl chloride (~11 mmol) in dry pyridine (12 mL), yielding a golden yellow gum. The products were separated by silica gel column chromatography to obtain racemic **12** (1.05 g, 48%) and **15** (0.080 g, 3%).

Data for **15**:

Mp: 201-204 ºC;**IR** (Nujol, cm^{-1}) ν: 1732, 1716; **^{1}H NMR** (400 MHz, $CDCl_3$): δ4.67-4.72 (2H, m) 5.01–5.06 (1H, m), 5.69-5.72 (1H, m), 5.74-5.77 (1H, m), 5.83-5.87 (2H, m), 6.93 (4H, t, *J* = 8.5 Hz), 7.19 (2H, t, *J* = 8.5 Hz), 7.86–7.93 (4H, m), 8.19-8.25 (2H, m) ppm;**^{13}C NMR** (50.3 MHz, $CDCl_3$): δ 63.9, 66.8, 68.6, 69.3, 103.3, 115.7 (d, $^2J_{C\text{-}F}$ = 22 Hz), 115.9 (d, $^2J_{C\text{-}F}$ = 22 Hz), 124.8 (d, $^4J_{C\text{-}F}$ = 3 Hz), 125.5 (d, $^4J_{C\text{-}F}$ = 2.5 Hz), 132.6 (t, $^3J_{C\text{-}F}$ = 9.9 Hz), 164.0, 165.3, 166.0 (d, $^1J_{C\text{-}F}$ = 256 Hz) ppm; **^{19}F NMR** (376.5 MHz, $CDCl_3$): -104.5 (1F, s), -104.0 (2F, s), -162.3 (C_6F_6) ppm; **Elemental analysis:** Calcd. for $C_{28}H_{19}O_9F_3$: C, 60.44; H, 3.44. Found: C, 60.43; H, 3.07 %.

2-*O*-(4-bromobenzoyl)-*myo*-inositol 1,3,5-orthoformate(**16**)**.**

myo-Inositol 1,3,5-orthoformate (0.570 g, 3 mmol) was acylated as described in the general procedure with 4-bromobenzoyl chloride (~ 7.5 mmol) in dry pyridine (7 mL). The mixture of products was silica gel column chromatographed to obtain racemic **10** (0.236 g, 14%) and **16 (**0.433 g, 39%).

Data for **16**:

Mp: 156-157 ºC; **IR** (Nujol, cm^{-1}) ν: 3550-3250, 1716; **^{1}H NMR** (200 MHz, $CDCl_3$): δ 4.03 (2H, d, *J* = 4.8 Hz), 4.36-4.42 (1H, m), 4.46-4.50 (2H, m), 4.61-4.72 (2H, m), 5.53-5.59 (2H, m), 7.62 (2H, dt, *J* = 8.5 and 2 Hz), 8.00 (2H, dt, *J* = 8.5 and 2 Hz) ppm; **^{13}C NMR** (50.3 MHz, CD_3COCD_3): δ69.4, 73.1, 74.3, 77.3, 107.6, 133.0, 134.5, 136.6, 137.1, 170.0 ppm; **Elemental analysis:** Calcd. for $C_{14}H_{13}O_7Br$: C, 45.06; H, 3.51. Found: C, 45.29; H, 3.61 %.

2-*O*-(4-chlorobenzoyl)-*myo*-inositol 1,3,5-orthoformate (**17**)**.**

myo-Inositol 1,3,5-orthoformate (0.760 g, 4 mmol) was acylated as described in the general procedure with 4-chlorobenzoyl chloride (~4 mmol) in dry pyridine (10 mL), yielding a yellow gum. The mixture of products was silica gel column chromatographed to obtain racemic **11** (0.278 g, 15%) and **17** (0.322 g, 25%).

Data for **17**:

Mp: 151-154 ºC; **IR** (Nujol, cm-1) ν: 3550-3300, 1716; **^{1}H NMR** (200 MHz, $CDCl_3$): δ4.04-4.13 (2H, m) 4.34-4.40 (1H, m), 4.42-4.47 (2H, m), 4.61-4.71 (2H, m), 5.52-5.57 (2H, m), 7.43 (2H, tt, *J* = 8.7 and 2 Hz), 8.05 (2H, tt, *J* = 8.7 and 2 Hz) ppm; **^{13}CNMR** (50.3 MHz, $CDCl_3$): δ64.0, 68.1, 68.6, 71.9, 102.5, 127.8, 128.9, 131.4, 140.3, 165.8 ppm; **Elemental analysis:** Calcd. for $C_{14}H_{13}O_7Cl$: C, 51.16; H, 3.99. Found: C,51.40; H, 3.82 %.

Details of crystal structure refinement

12•CH_3COCH_3

The terminal carbon atoms of the guest acetone molecule are disordered over two positions, the occupancies of the fragments were determined by refining them against a free variable with their sum set as 1. SADI restraints were applied to maintain chemically reasonable bond lengths in the fragments. The thermal anisotropies of the disordered atoms were restrained using RIGU and SIMU instructions.

12•CH_2Cl_2

The carbon atom and one of the chlorine atoms of the dichloromethane molecule are disordered over two positions with equal occupancies. SADI restraints were applied to maintain chemically reasonable bond lengths in the fragments. The thermal anisotropies of the disordered atoms were restrained using RIGU instructions. The ADPs of the two positions of the disordered carbon atom were constrained to the same value using the EADP command.

12•CH_3NO_2

The nitromethane molecule is disordered over three positions, the occupancies of which are 0.55, 0.30 and 0.15. The O-N and C-N distances were constrained to values of 1.22 Å and 1.48 Å using a DFIX command. SADI restraints were applied to maintain chemically reasonable bond lengths in the fragments. The ADPs of two positions of the disordered oxygen and nitrogen atoms were constrained to the same value using the EADP command. The thermal anisotropies of the disordered C, N and O atoms were restrained using DELU instructions.

12•CCl_4

The four chlorine atoms in the carbon tetrachloride molecule are disordered over two positions, the occupancies of which were determined by refining them against a free variable with their sum set as 1. SADI restraints were applied to the C-Cl bond lengths to maintain chemically reasonable geometry.

12•CH_3SOCH_3

The carbon and sulfur atoms of the included dimethyl sulfoxide molecule are disordered over four positions with equal occupancy. The C-S and S-O distances were constrained to values of 1.77 Å and 1.5 Å using DFIX commands. The C-C distances in each fragment were constrained to a value of 2.7 Å using a DFIX command. The ADPs of two positions of the disordered carbon and sulfur atoms were constrained to the same value using the EADP command.

12•$C_2H_4Cl_2$

The included dichloroethane molecule was disordered over two positions, with the position of one of the chlorine atoms (Cl1) common. The occupancies of the sites were determined by refining them against a free variable with their sum set as 1. The C-C bond length in $ClCH_2CH_2Cl$ molecule were restrained to 1.5 Å using a DFIX instruction.

12•*o*-$C_6H_4(CH_3)_2$

The *o*-xylene molecule is disordered over two positions. The occupancies of the sites were determined by refining them against a free variable with their sum set as 1. The C-C bond lengths (distance between the methyl and aromatic carbon atoms) in each fragment were constrained to a value of 1.51 Å using a DFIX command and SADI restraints were applied to maintain chemically reasonable geometry in the fragments. The thermal anisotropies of the disordered atoms were restrained using RIGU and SIMU instructions.

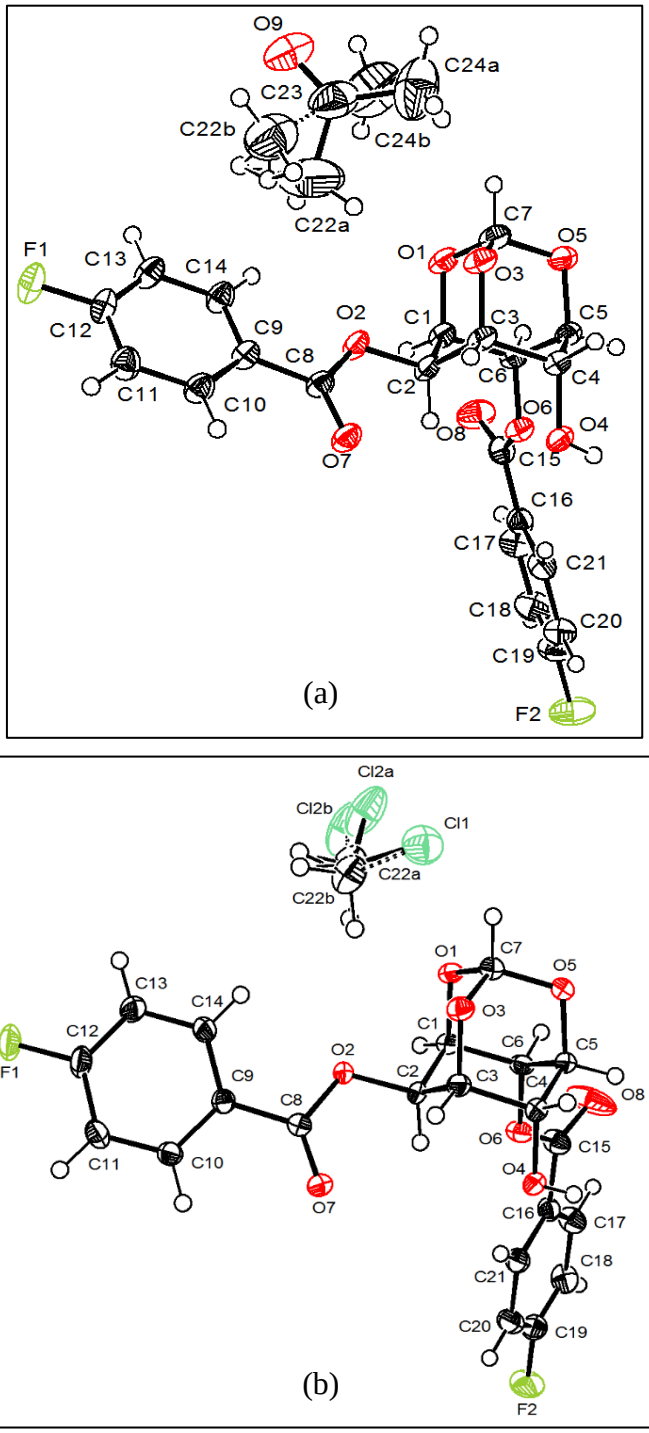

Figure S1. ORTEPs for solvatomorphs of **12**: (a) **12**•CH_3COCH_3 and (b) **12**•CH_2Cl_2. Thermal ellipsoids are drawn at 50% probability and hydrogen atoms are depicted as small spheres of arbitrary radii. The bonds of the minor component in disordered molecules are shown as dashed lines.

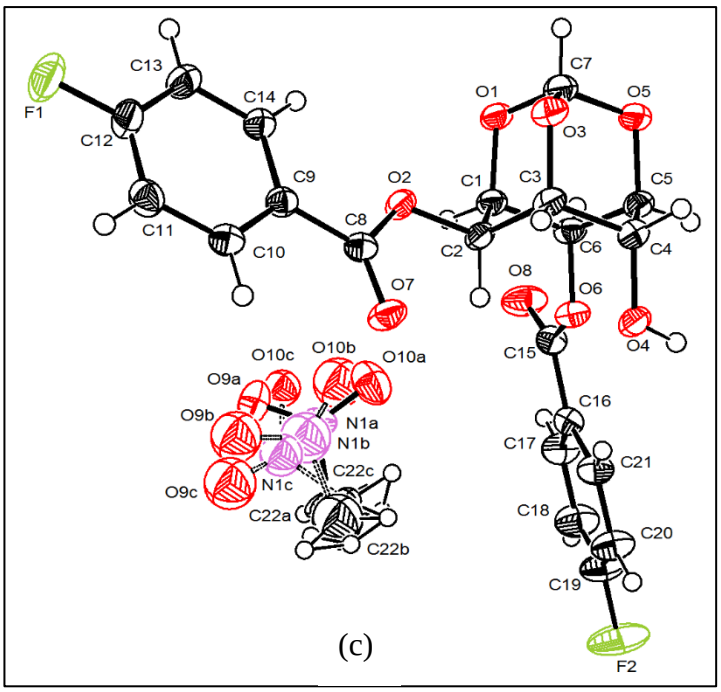

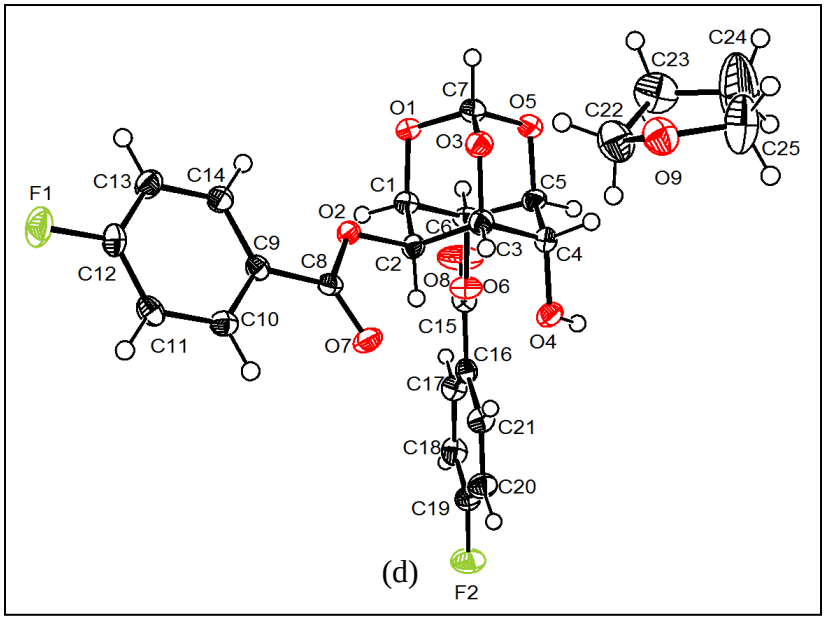

Figure S1 (contd). ORTEPs for solvatomorphs of **12**: (c) **12**•CH_3NO_2 and (d) **12**•C_4H_8O. Thermal ellipsoids are drawn at 50% probability and hydrogen atoms are depicted as small spheres of arbitrary radii. The bonds of the minor component in disordered molecules are shown as dashed lines.

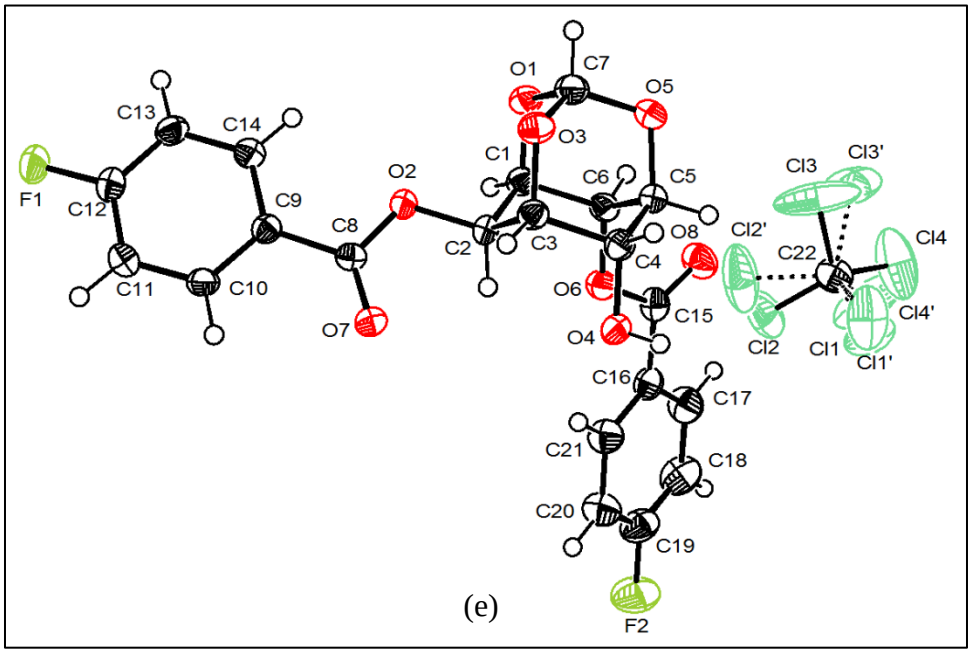

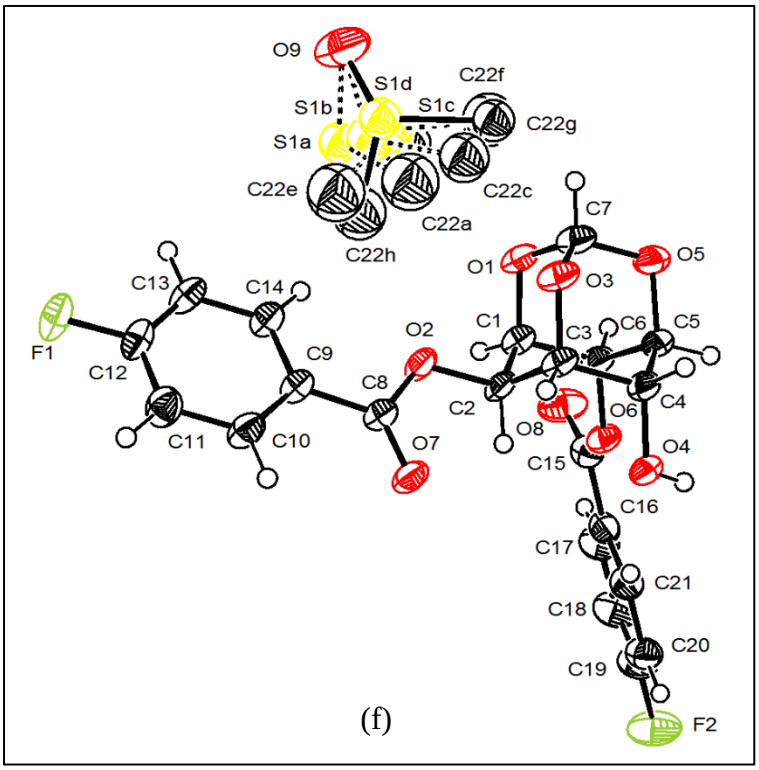

Figure S1 (contd). ORTEPs for solvatomorphs of **12**: (e) **12**•CCl_4 and (f) **12**•CH_3SOCH_3. Thermal ellipsoids are drawn at 50% probability and hydrogen atoms are depicted as small spheres of arbitrary radii. The bonds of the minor component in disordered molecules are shown as dashed lines. Hydrogen atoms of the disordered DMSO molecules are omitted for clarity.

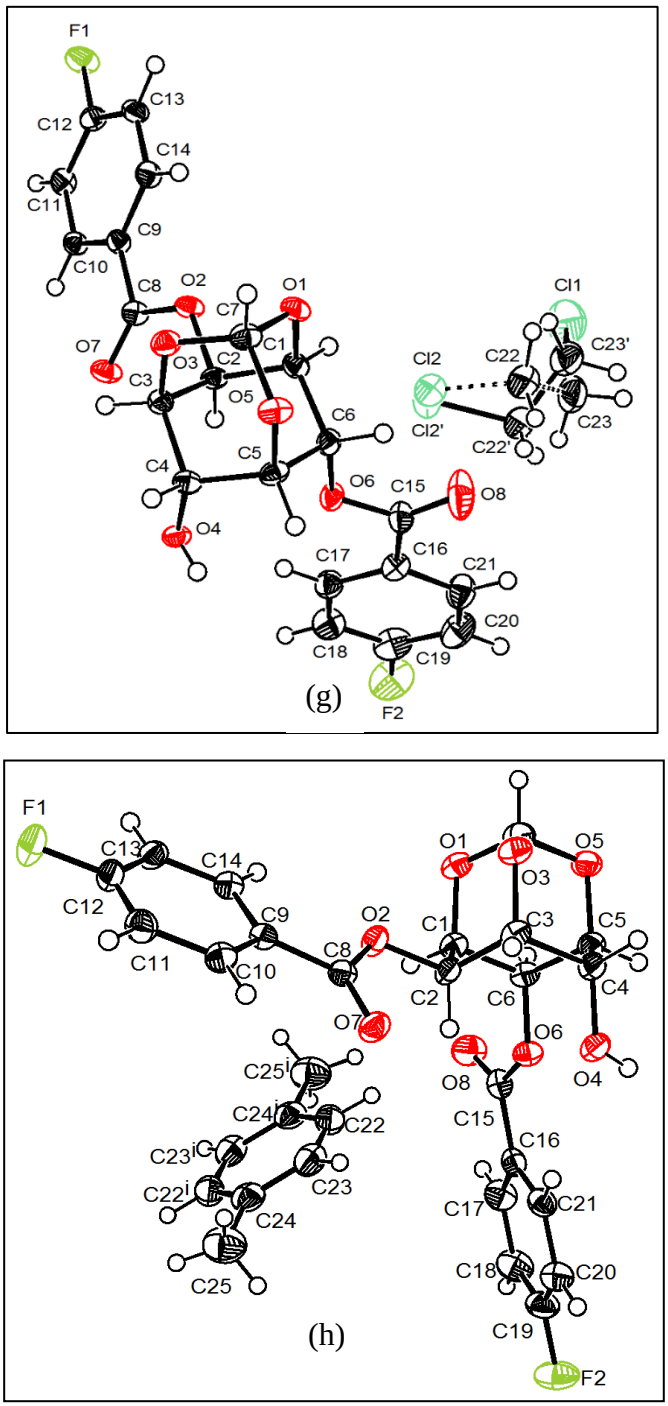

Figure S1 (contd). ORTEPs for solvatomorphs of **12**: (g) **12**•$C_2H_4Cl_2$ and (h) **12**•*p*-$C_6H_4(CH_3)_2$. Thermal ellipsoids are drawn at 50% probability and hydrogen atoms are depicted as small spheres of arbitrary radii. The bonds of the minor component in disordered molecules are shown as dashed lines.

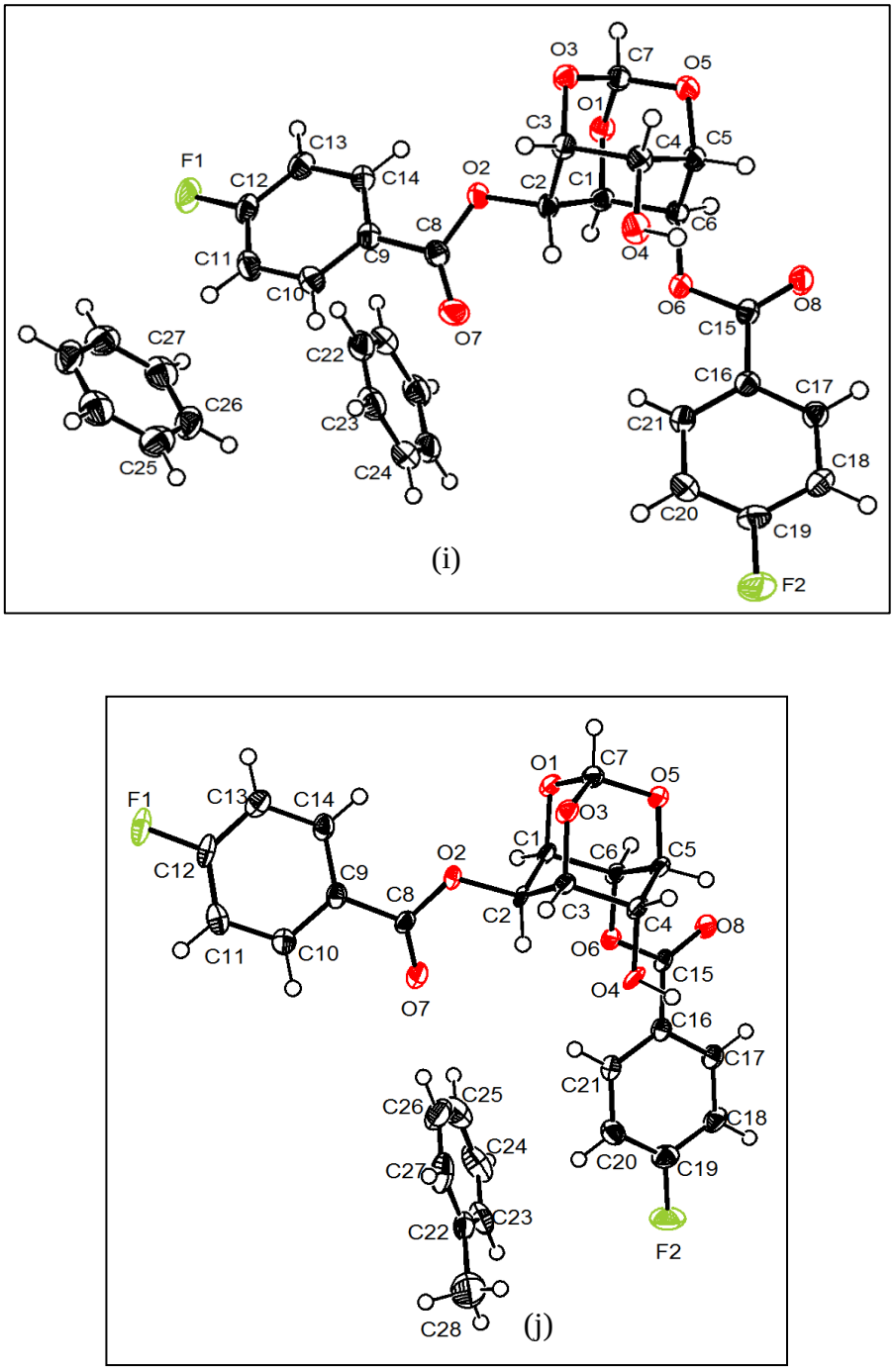

Figure S1 (contd). ORTEPs for solvatomorphs of **12**: (i) **12**•C_6H_6 and (j) **12**•$C_6H_5CH_3$. Thermal ellipsoids are drawn at 50% probability and hydrogen atoms are depicted as small spheres of arbitrary radii.

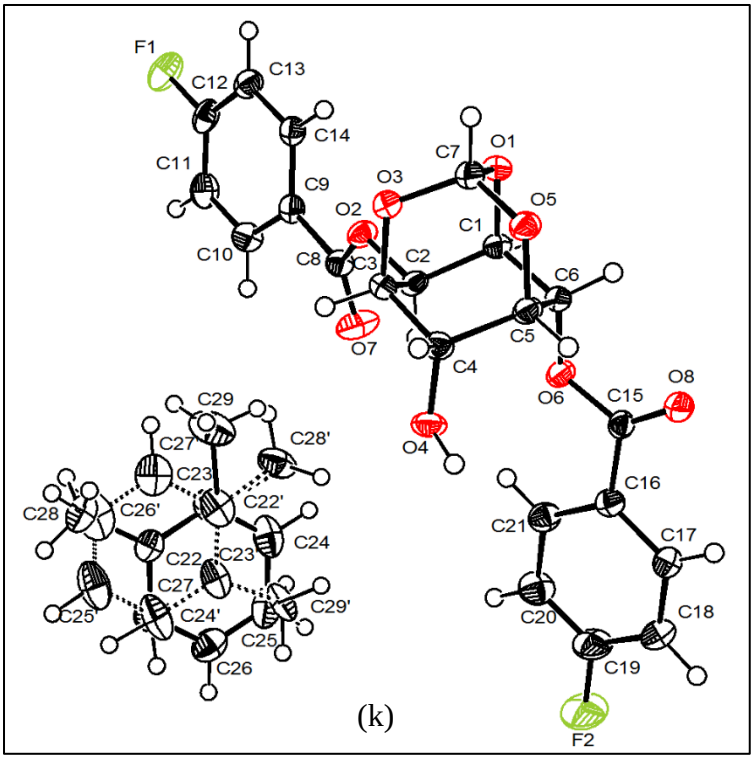

Figure S1 (contd). ORTEPs for solvatomorphs of **12**: (k) **12**•*o*-$C_6H_4(CH_3)_2$. Thermal ellipsoids are drawn at 50% probability and hydrogen atoms are depicted as small spheres of arbitrary radii. The bonds of the minor component in disordered molecules are shown as dashed lines.

Differential Scanning Calorimetry (DSC)

The thermal behavior of freshly grown crystals was investigated by measuring enthalpy change on a Mettler differential scanning calorimeter. Freshly grown crystals (2-4 mg) were placed in a sealed aluminium pan (40 µl) and were analyzed from ambient temperature to ~ 35 ºC above the melting point of the compound using an empty pan as the reference. The heating rate was 5 ºC min^{-1} (or 10 ºC min^{-1} in some experiments) and nitrogen gas was used for purging.

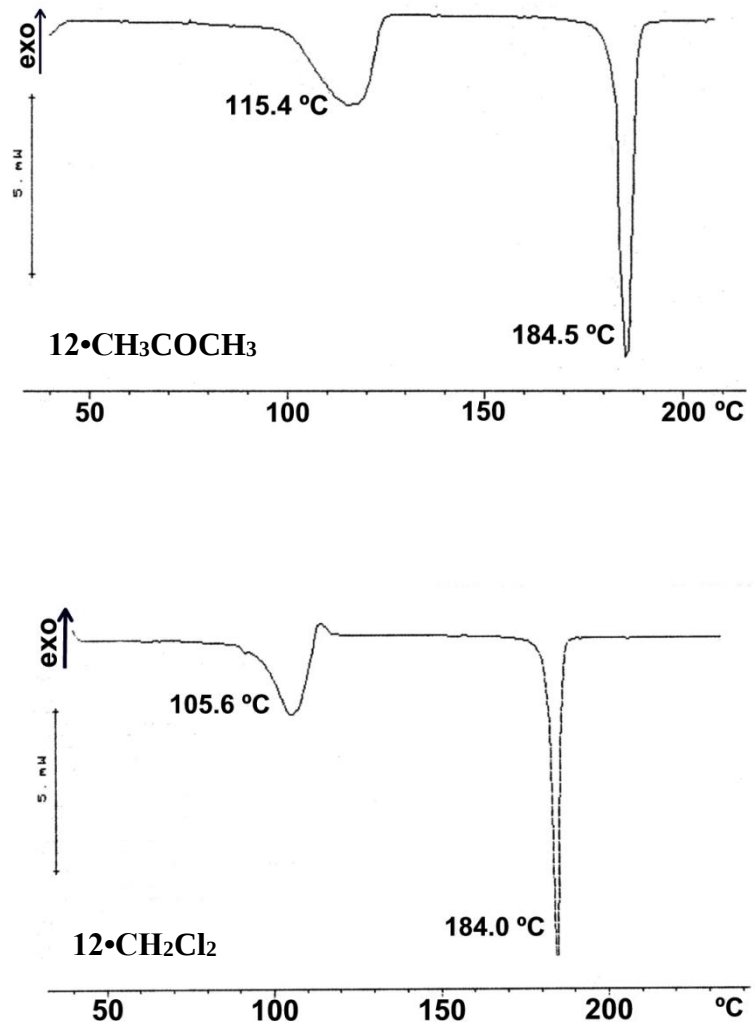

Figure S2. DSC curves for solvatomorphs of **12**.

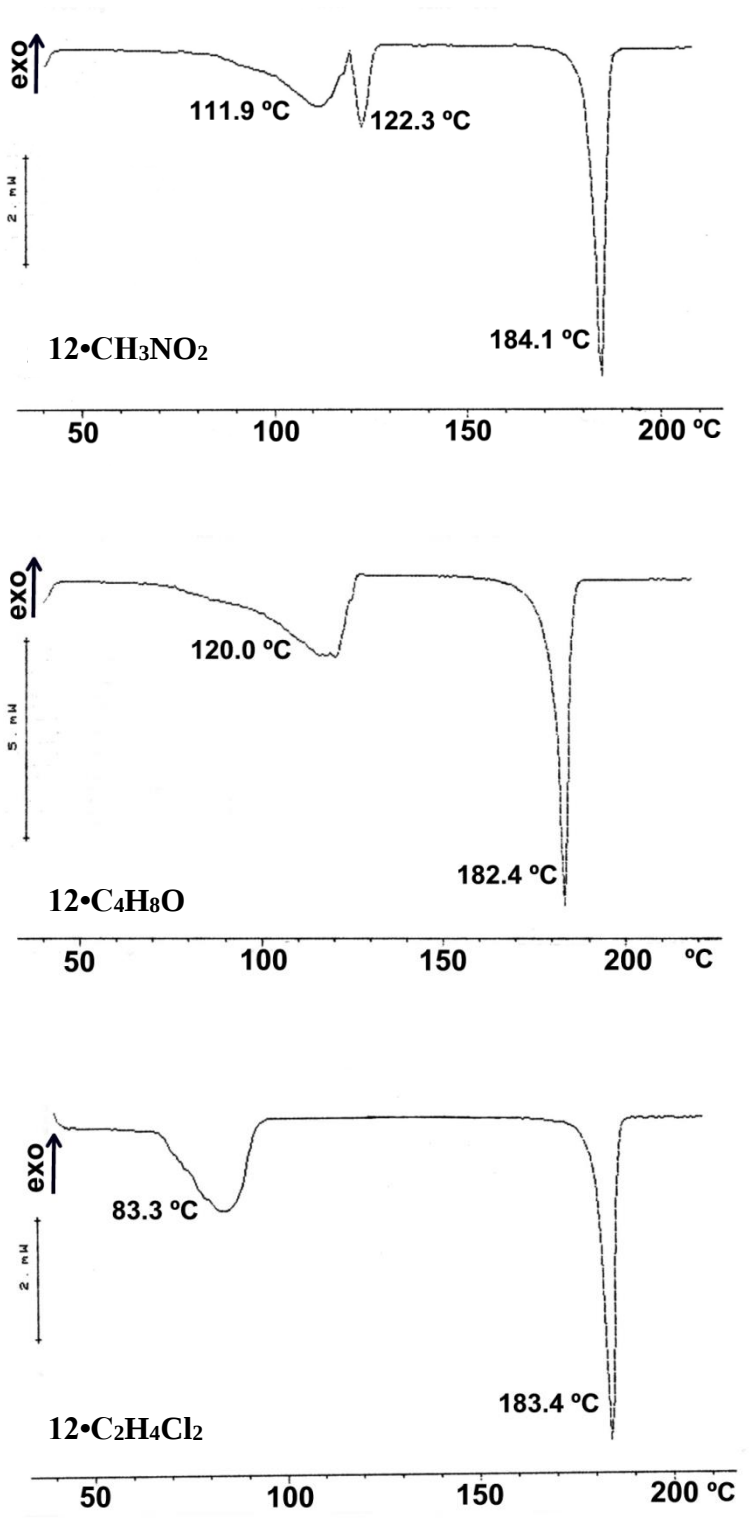

Figure S2 (contd). DSC curves for solvatomorphs of **12**.

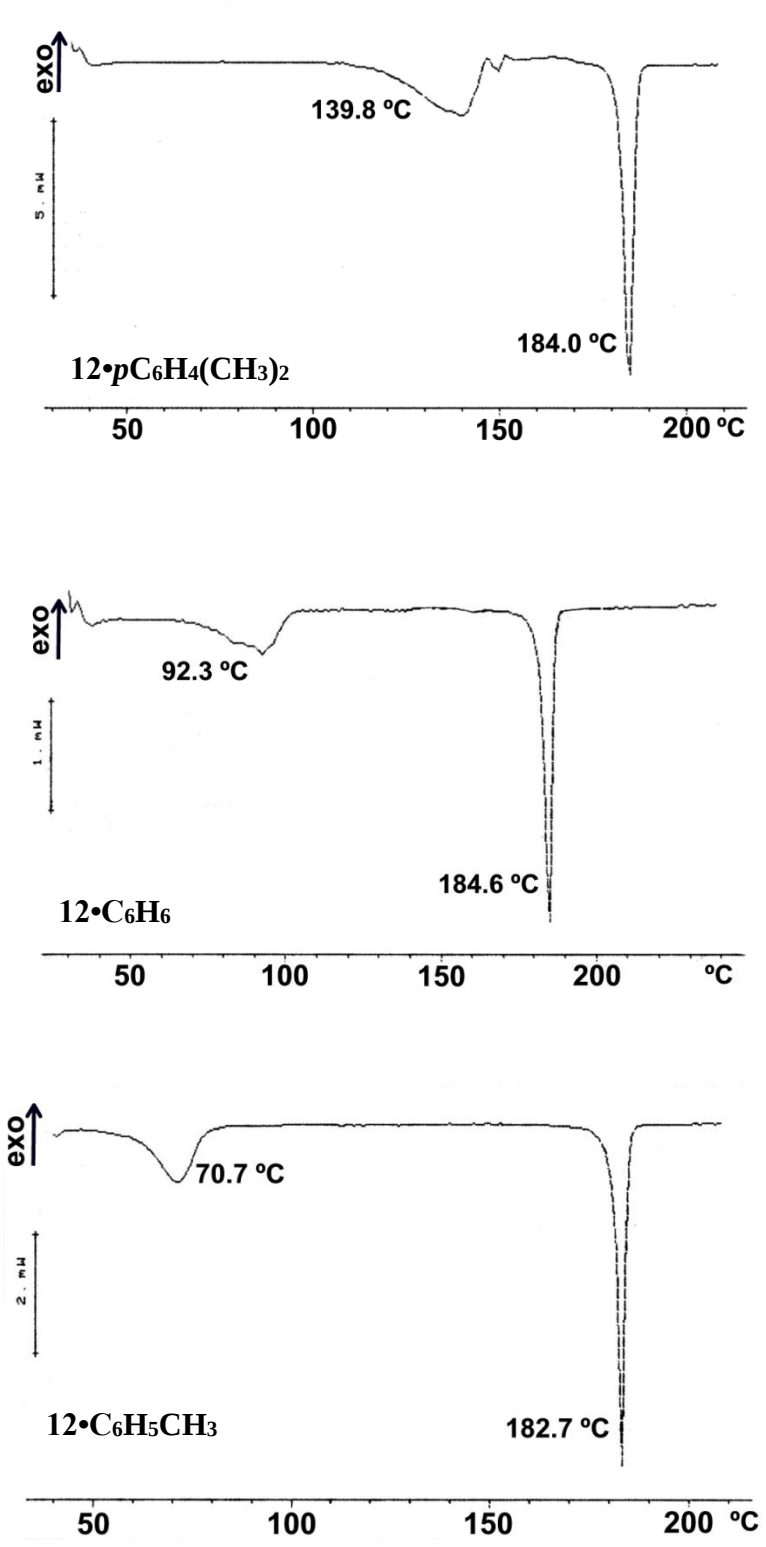

Figure S2 (contd). DSC curves for solvatomorphs of **12**.

Hot stage microscopy (HSM)

Crystals were heated on the stage (equipped with a temperature probe) and viewed through the eyepiece of a Leica polarizing microscope. Their images were captured using an on-board Leica camera.

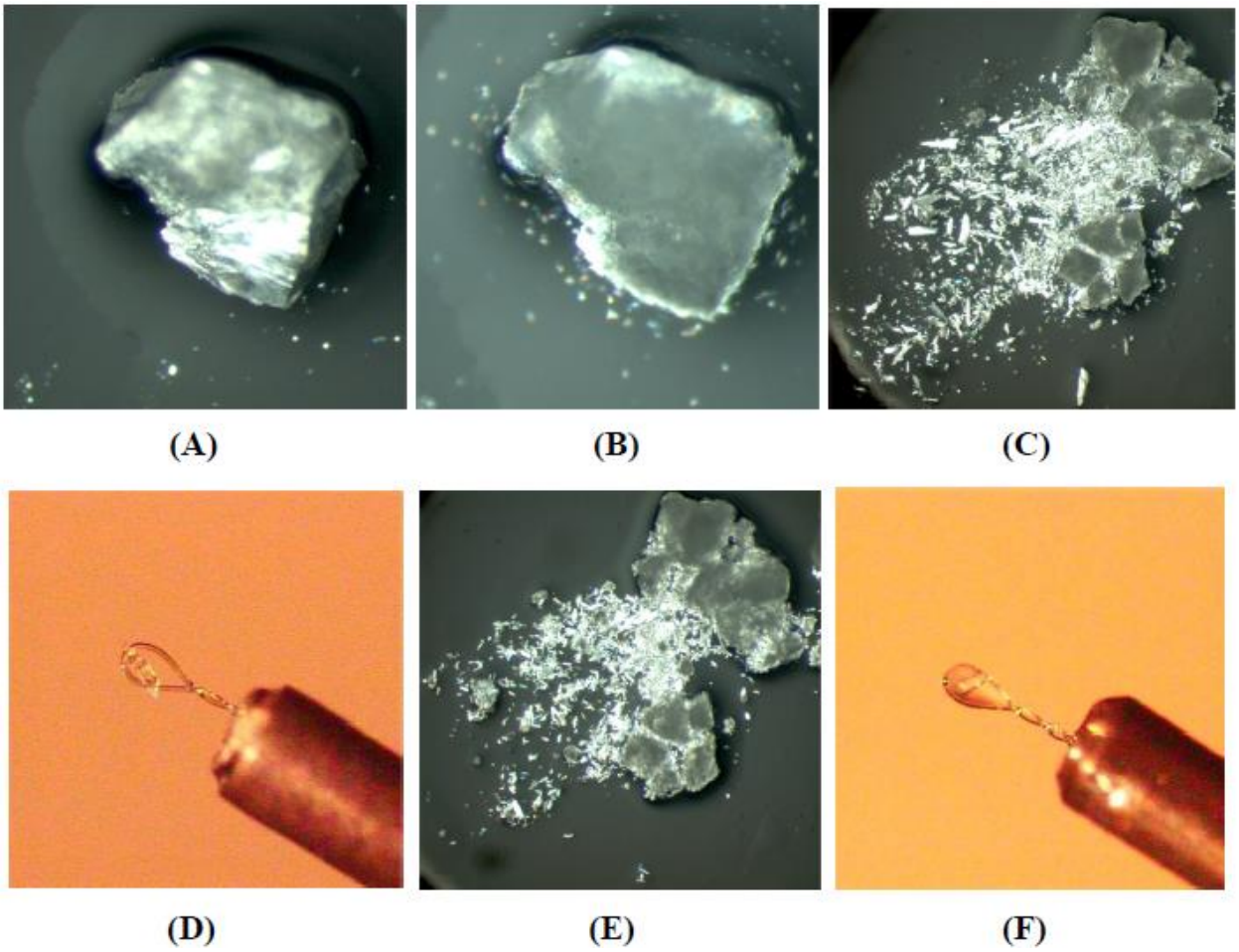

Figure S3. Hot stage microscopy images for **11**•CH_3NO_2: (A) 100 °C: onset of solvent escape; (B) 140 °C: loss of solvent and crystallinity; (C) smaller crystalline fragments obtained from larger opaque crystal; (D) unit cell determination: solvent-free form I crystal (**11**•FI); (E) fragments in (C) reheated to 220 °C; (F) plate-like solvent-free form II crystals (**11**•FII).

^{19}F NMR spectrum (in $CDCl_3$+ C_6F_6) of racemic 2,6-di-*O*-(4-fluorobenzoyl)-*myo*-inositol 1,3,5-orthoformate (**12**).

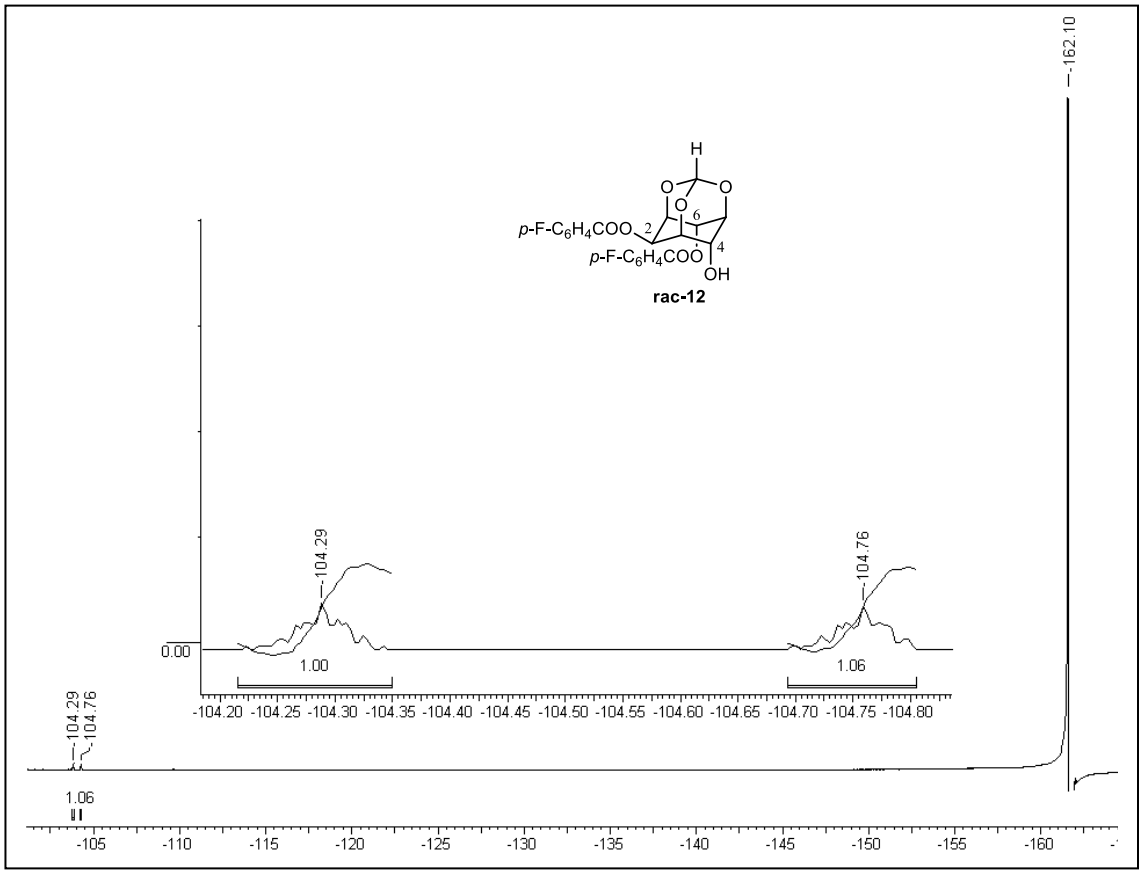

^{19}F NMR spectrum (in $CDCl_3$ + C_6F_6) of 2,4,6-tri-O-(4-fluorobenzoyl)-*myo*-inositol 1,3,5-orthoformate **15.**

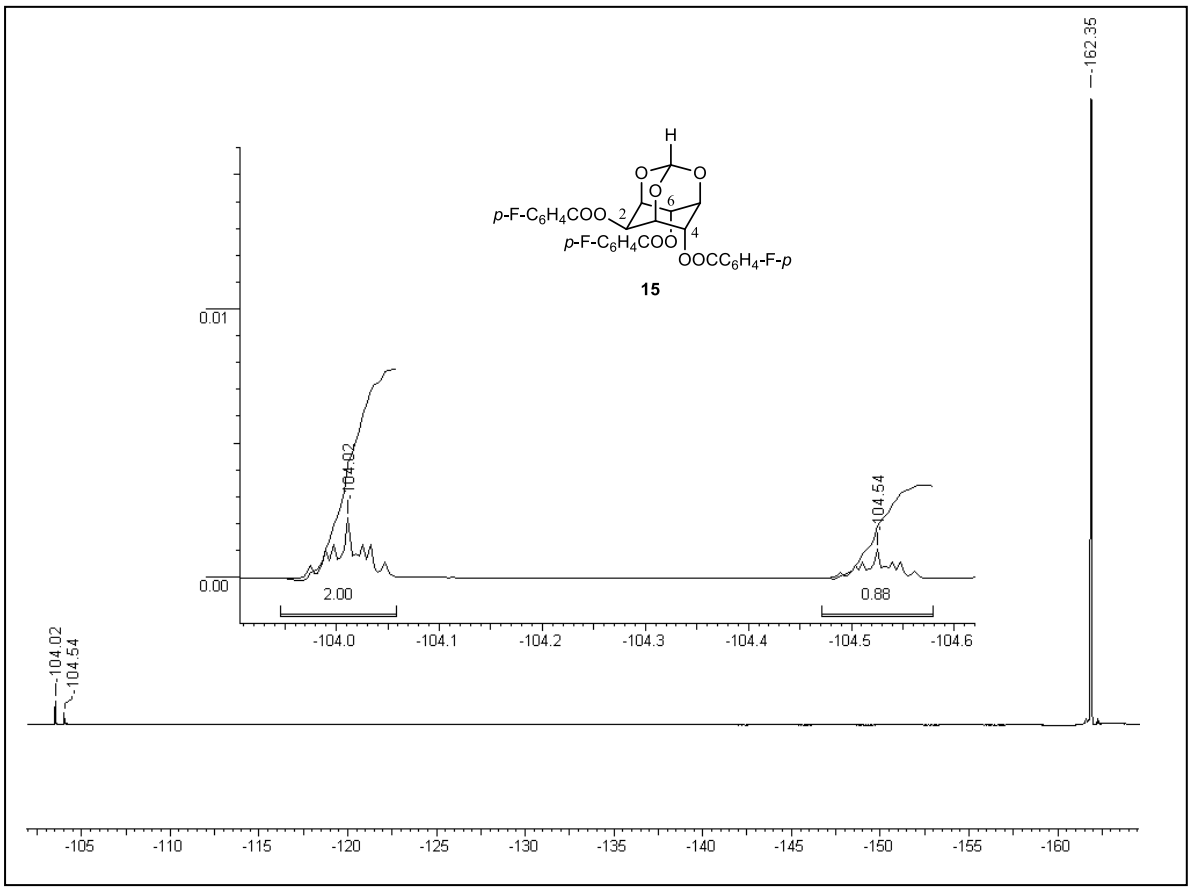

^{19}F NMR spectrum (in CD_3SOCD_3 + C_6F_6) of 2-O-(4-fluorobenzoyl)-*myo*-inositol 1,3,5-orthoformate **18.**

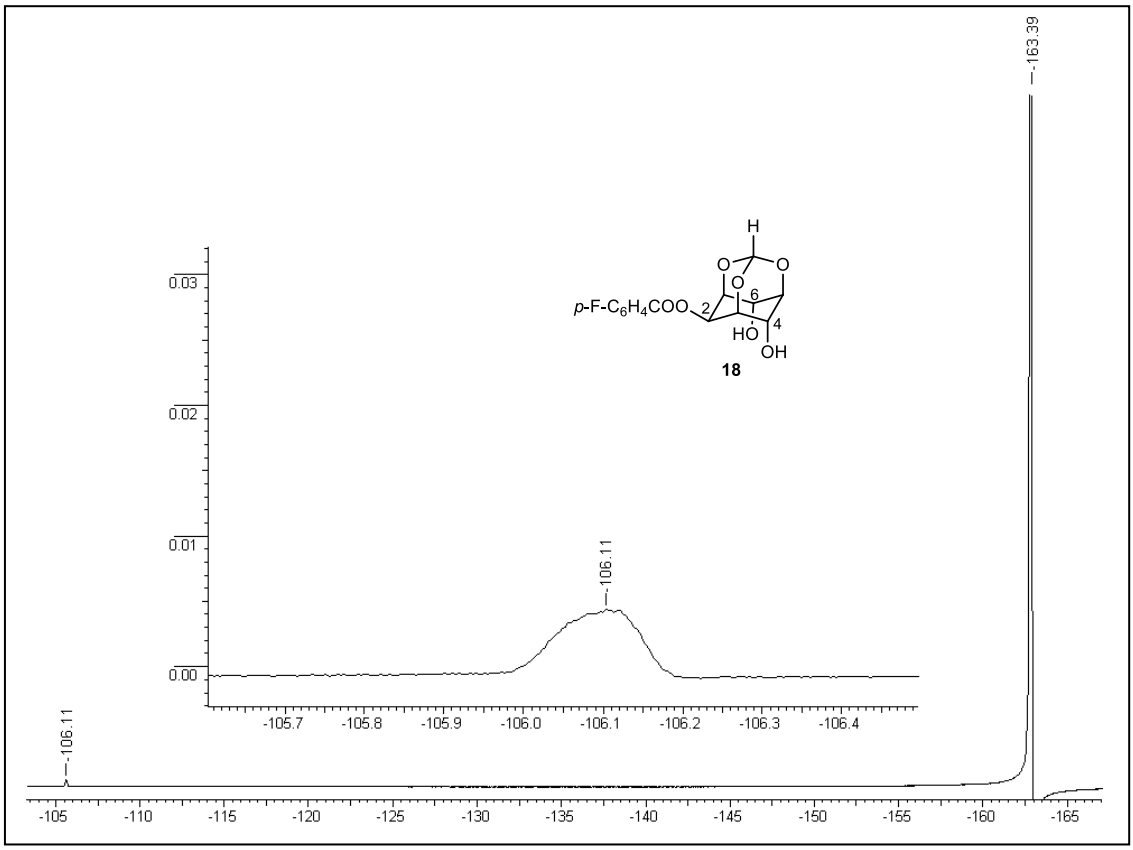

^{19}F NMR spectrum (in $CDCl_3$ + CD_3SOCD_3 + C_6F_6) of product mixture of the solid-state reaction of **12**•CH_3NO_2**.**

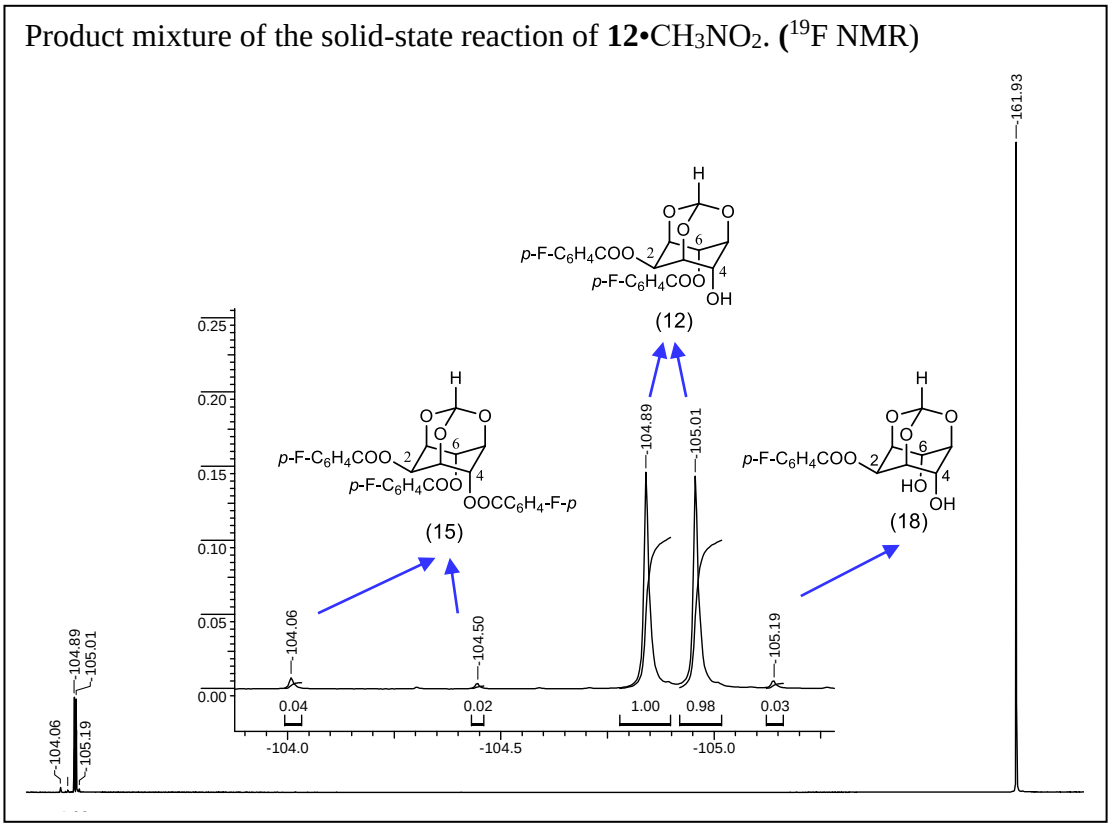

^{19}F NMR spectrum (in $CDCl_3$ + CD_3SOCD_3 + C_6F_6) of product mixture of the solid-state reaction of **12**•FI**.**

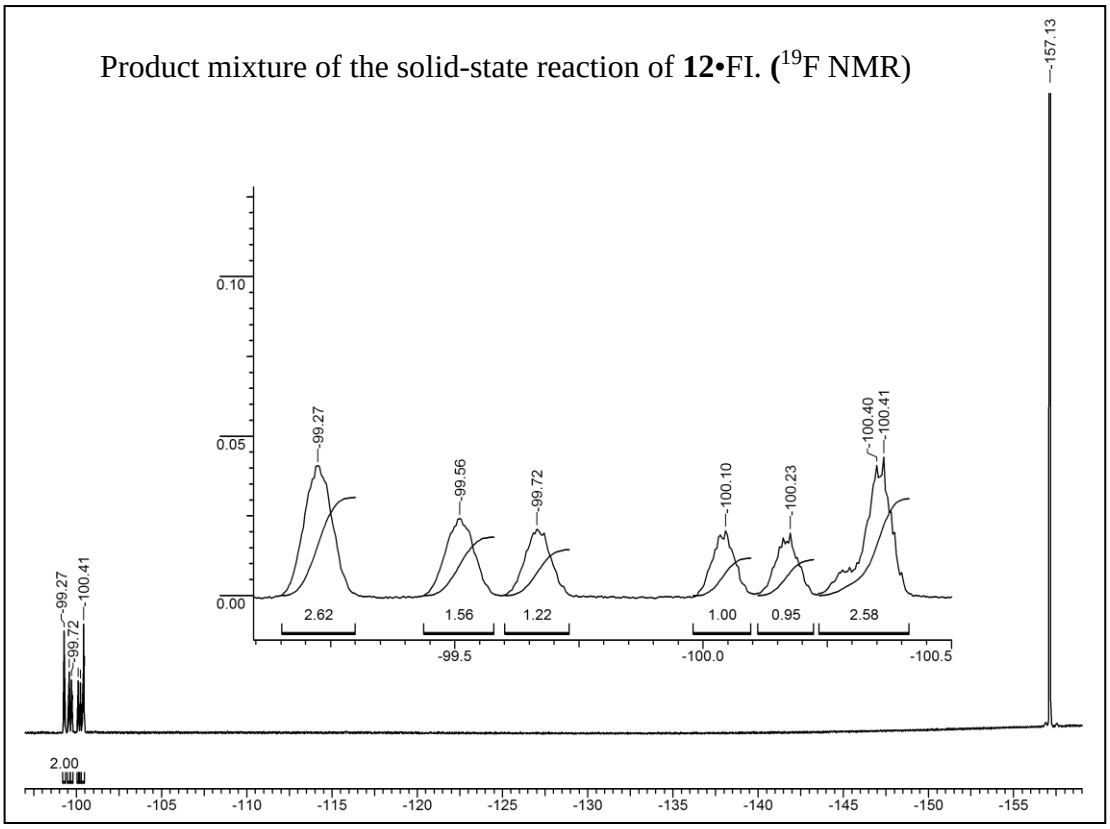

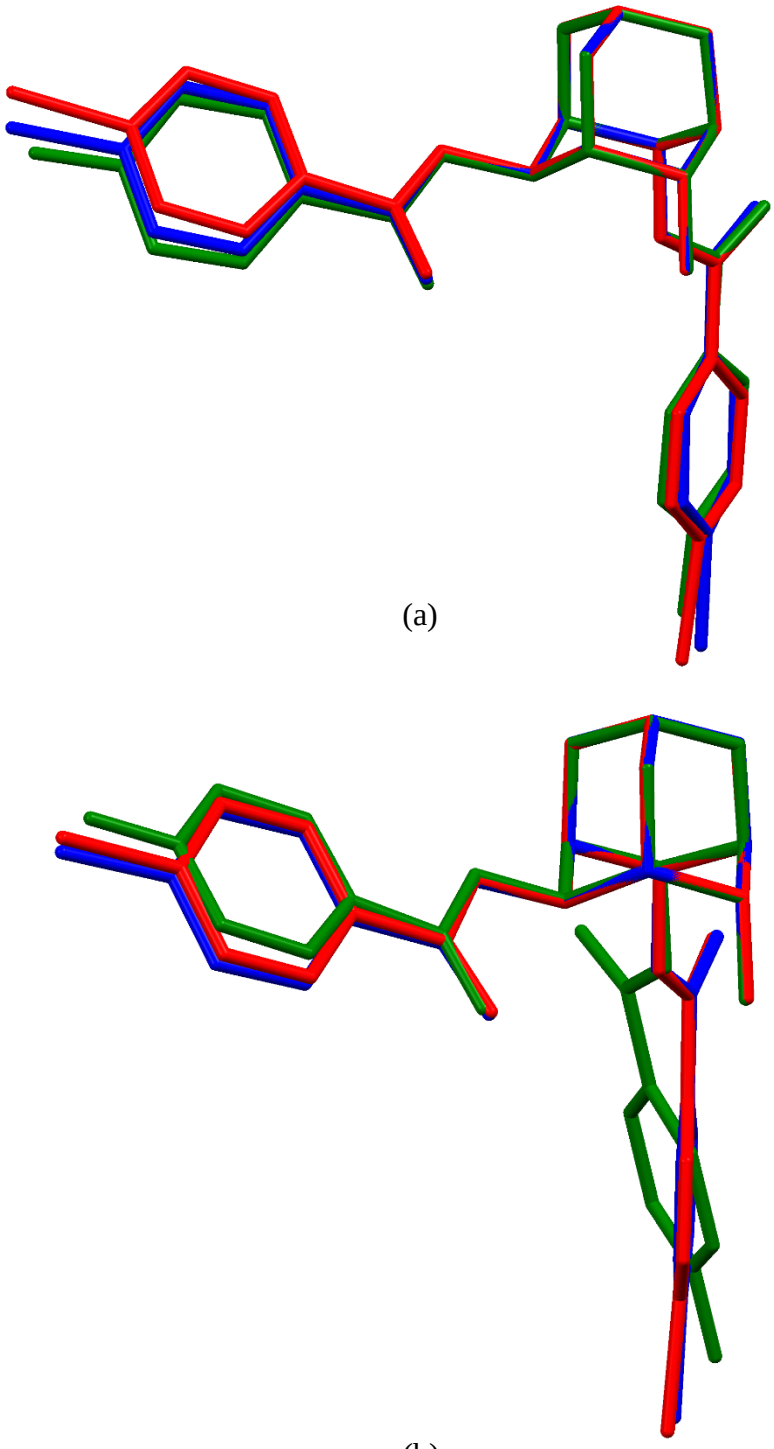

Figure S4. The molecular overlap of host molecules in (a) **10**•$CHCl_3$ (red), **11**•$CHCl_3$ (blue) and **12**•$CHCl_3$ (green) and (b) **10**•CH_3COCH_3 (red), **11**•CH_3COCH_3 (blue) and **12**•CH_3COCH_3 (green).

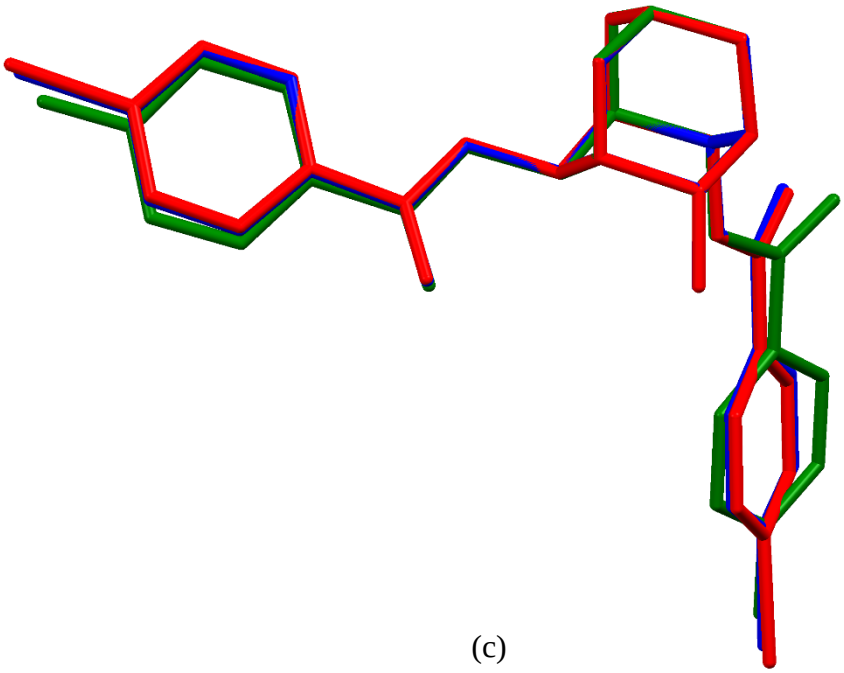

(c)

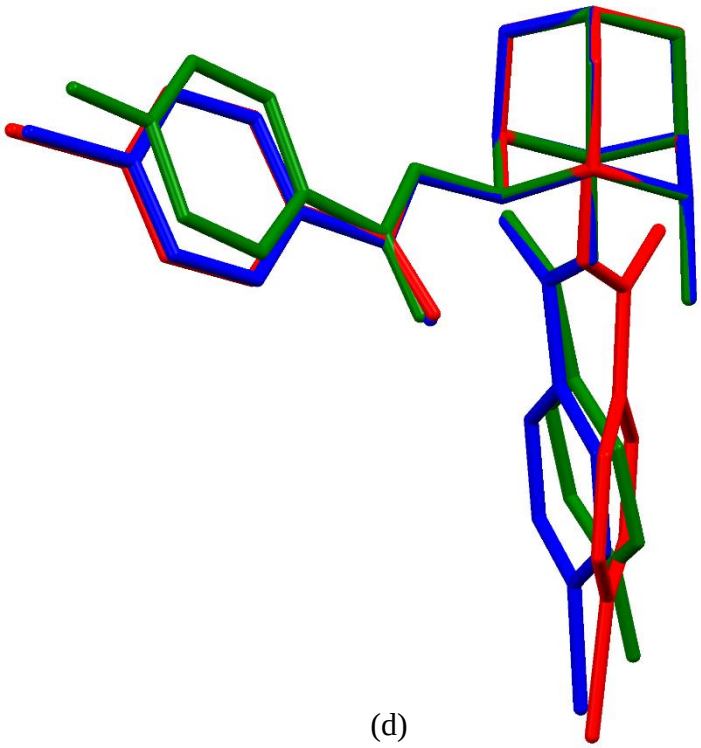

(d)

Figure S4 (contd). The molecular overlap of host molecules in (c) **10**•CH_2Cl_2 (red), **11**•CH_2Cl_2 (blue) and **12**•CH_2Cl_2 (green) and (d) **10**•CH_3NO_2 (red), **11**•CH_3NO_2 (blue) and **12**•CH_3NO_2 (green).

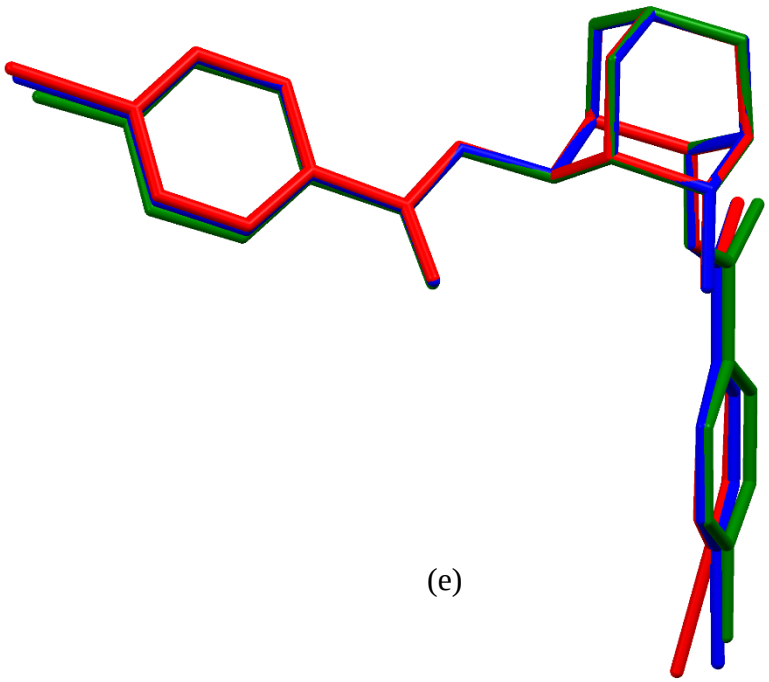

(e)

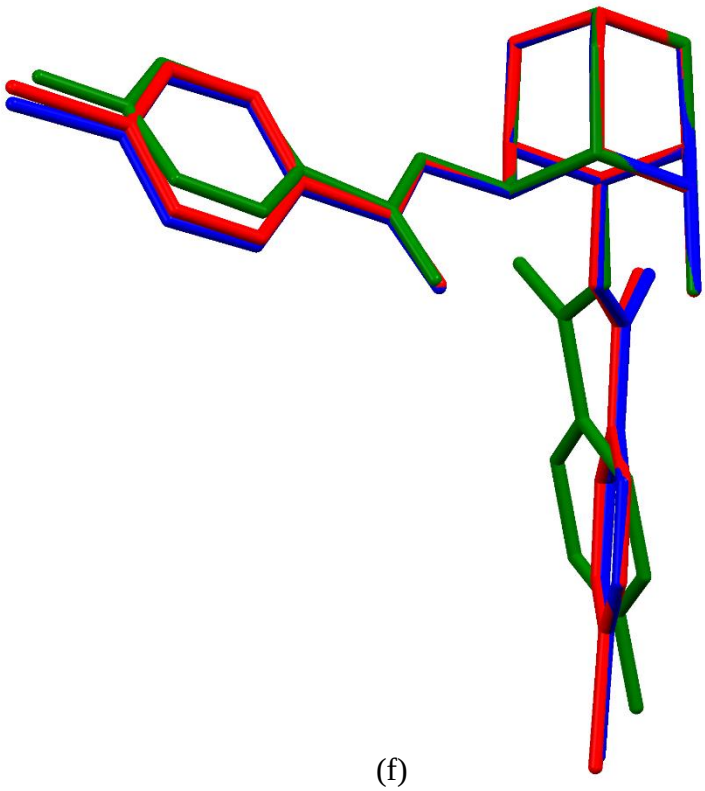

(f)

Figure S4 (contd). The molecular overlap of host molecules in (e) **10**•C_4H_8O(red), **11**• C_4H_8O(blue) and **12**• C_4H_8O(green) and (f) **10**•$(CH_3)_2SO$(red), **11**•$(CH_3)_2SO$(blue) and **12**•$(CH_3)_2SO$(green).

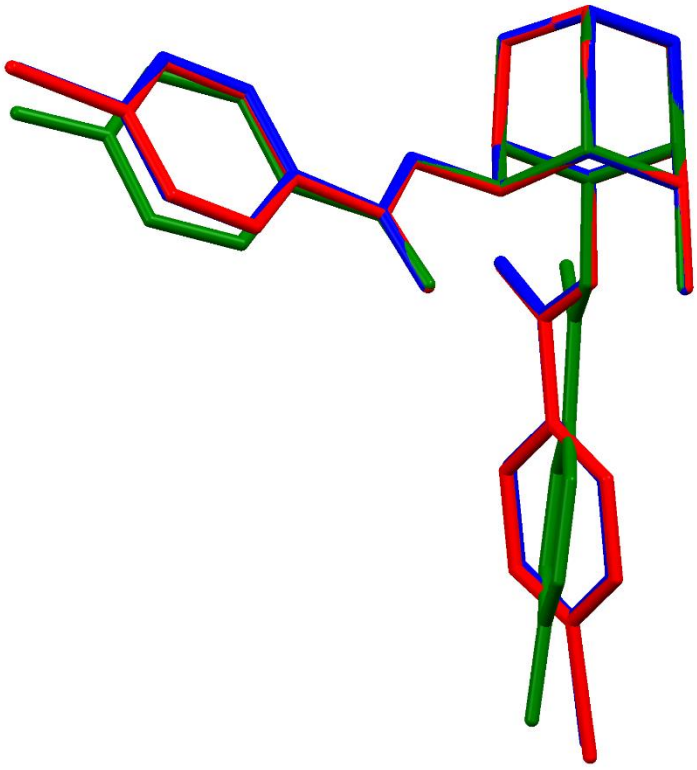

(g)

Figure S4 (contd). The molecular overlap of host molecules in (g) **10**•$ClCH_2CH_2Cl$(red), **11**•$ClCH_2CH_2Cl$(blue) and **12**•$ClCH_2CH_2Cl$(green).

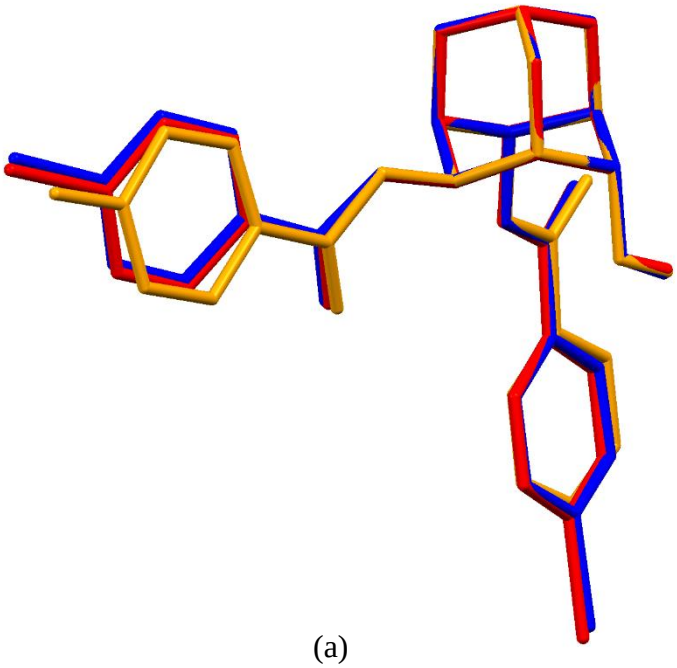

(a)

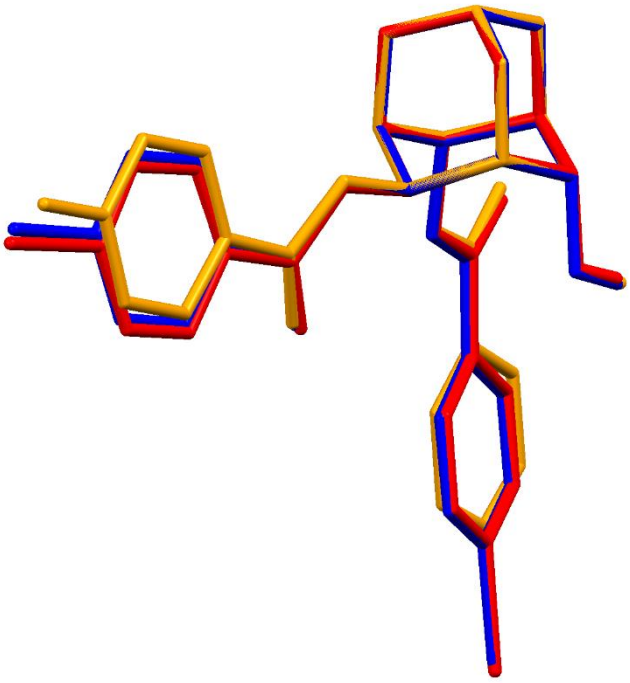

(b)

Figure S5. The overlap of molecules in crystals of **12**•FI (yellow) with (a) Form I solvent free crystals of **10** (blue) and **11** (red) and (b) Form II solvent free crystals of **10** (blue) and **11** (red).

Table S1. Intermolecular interactions build helices in group I and bilayers in group II crystals.

Group I	D-H…A	D-H (Å)	H-A (Å)	D-A (Å)	∠D-H…A (°)	Symmetry codes
12•$CHCl_3$	O4-H4A⋯O7	0.77(4)	2.04(4)	2.803(3)	172(4)	*-x* + 3/2, *y* - 1/2, *-z* + 1/2
	C5-H5⋯O4	1.00	2.53	3.243(4)	128	*-x* + 3/2, *y* - 1/2, *-z* + 1/2
	C11-H11⋯O1	0.95	2.47	3.329(3)	150	*x*, *y* + 1, *z*
12•CH_3COCH_3	O4-H4A⋯O7	0.83(3)	1.98(3)	2.804(2)	178(4)	*-x* + 2, *y* - 1/2, *-z* + 1/2
	C5-H5⋯O4	1.00	2.62	3.269(3)	123	*-x* + 2, *y* - 1/2, *-z* + 1/2
	C11-H11⋯O1	0.95	2.53	3.224(3)	130	*x*, *y* + 1, *z*
12•CH_2Cl_2	O4-H4A⋯O7	0.79(3)	2.01(3)	2.7931(19)	169(3)	*-x* + 3/2, *y* - 1/2, *-z* + 1/2
	C5-H5⋯O4	1.00	2.49	3.196(2)	128	*-x* + 3/2, *y* - 1/2, *-z* + 1/2
	C11-H11⋯O1	0.95	2.54	3.367(2)	145	*x*, *y* + 1, *z*
12•CH_3NO_2	O4-H4A⋯O7	0.87(3)	1.94(3)	2.803(2)	172(3)	*-x* + 1, *y* – ½, *-z* + 1/2
	C5-H5⋯O4	1.00	2.62	3.290(2)	125	*-x* + 1, *y* – ½, *-z* + 1/2
	C11-H11⋯O1	0.95	2.60	3.302(2)	131	*x*, *y* + 1, *z*
12•C_4H_8O	O4-H4A⋯O7	0.89(3)	1.90(3)	2.789(2)	173(3)	*-x* + ½, *y* – ½, *-z* + 1/2
	C5-H5⋯O4	1.00	2.62	3.354(3)	131	*-x* + ½, *y* – ½, *-z* + 1/2
	C11-H11⋯O1	0.95	2.56	3.412(3)	149	*x*, *y* + 1, *z*
12•CCl_4	O4-H4A⋯O7	0.83(3)	1.99(3)	2.812(2)	171(3)	*-x* + 1/2, *y* - 1/2, *-z* + 3/2
	C5-H5⋯O4	1.00	2.60	3.337(3)	131	*-x* + 1/2, *y* - 1/2, *-z* + 3/2
	C11-H11⋯O1	0.95	2.68	3.536(3)	150	*x*, *y* + 1, *z*
12•CH_3SOCH_3	O4-H4A⋯O7	0.83(4)	1.97(4)	2.795(3)	176(3)	*-x* + 1, *y* + ½, *-z* + 1/2
	C5-H5⋯O4	1.00	2.62	3.249(3)	121	*-x* + 1, *y* + ½, *-z* + 1/2
	C11-H11⋯O1	0.95	2.55	3.245(3)	130	*x*, *y* - 1, *z*
12•$ClCH_2CH_2Cl$	O4-H4A⋯O7	0.71(3)	2.11(3)	2.816(3)	171(3)	*-x* + ½, *y* – ½, *-z* + 3/2
	C5-H5⋯O4	1.00	2.52	3.232(3)	128	*-x* + ½, *y* – ½, *-z* + 3/2
	C11-H11⋯O1	0.95	2.51	3.331(3)	145	*x*, *y* + 1, *z*
12•*p*-$C_6H_4(CH_3)_2$	O4-H4A⋯O7	0.85(2)	1.98(2)	2.8193(14)	169.5(18)	*-x*, *y* + ½, *-z* + 1/2
	C5-H5⋯O4	1.00	2.72	3.3560(18)	121	*-x*, *y* + ½, *-z* + 1/2
	C11-H11⋯O1	0.95	2.56	3.2230(18)	127	*x*, *y* – 1, *z*

Table S1 (contd). Intermolecular interactions build helices in group I and bilayers in group II crystals

Group II	D-H…A	D-H (Å)	H-A (Å)	D-A (Å)	∠D-H…A (°)	Symmetry codes
12•FI	O4-H4A⋯O1	0.86(3)	1.99(3)	2.8361(19)	167(2)	*x*, *y* + 1, *z*
	C1-H1⋯Cg6	0.98	2.61	3.549(2)	161	*x*, *y* – 1, *z*
	C5-H5⋯O8	0.98	2.52	3.380(3)	146	-*x* + 1, -*y* + 2, -*z*
	C6-H6⋯O5	0.98	2.43	3.400(2)	173	-*x* + 1, -*y* + 1, -*z*
	C7-H7⋯O8	0.98	2.45	3.192(3)	132	-*x* + 1, -*y* + 1, -*z*
	C14-H14⋯O4	0.93	2.44	3.332(3)	162	*x*, *y* – 1, *z*
12•C_6H_6	O4-H4A⋯O1	0.88(2)	1.92(2)	2.7882(13)	170.4(18)	*x* – 1, *y*, *z*
	C1-H1⋯Cg6	1.00	2.49	3.4411(15)	160	*x* + 1, *y*, *z*
	C5-H5⋯O8	1.00	2.46	3.2924(17)	141	-*x*, -*y* + 2, -*z*
	C6-H6⋯O5	1.00	2.41	3.3987(17)	170	-*x* + 1, -*y* + 2, -*z*
	C7-H7⋯O8	1.00	2.48	3.2482(17)	133	-*x* + 1, -*y* + 2, -*z*
	C14-H14⋯O4	0.95	2.36	3.2864(18)	165	*x* + 1, *y*, *z*
12•$C_6H_5CH_3$	O4-H4A⋯O1	0.84(3)	2.00(3)	2.830(3)	167(3)	*x* + 1, *y*, *z*
	C1-H1⋯Cg6	1.00	2.52	3.474(3)	160	*x* – 1, *y*, *z*
	C5-H5⋯O8	1.00	2.47	3.314(3)	142	-*x* + 1, -*y*, -*z*
	C6-H6⋯O5	1.00	2.43	3.424(3)	173	-*x*, -*y*, -*z*
	C7-H7⋯O8	1.00	2.54	3.264(3)	129	-*x*, -*y*, -*z*
	C14-H14⋯O4	0.95	2.45	3.376(4)	165	*x* – 1, *y*, *z*
12•*o*-$C_6H_4(CH_3)_2$	O4-H4A⋯O1	0.87(2)	1.96(2)	2.8176(15)	169(2)	*x* - 1, *y*, *z*
	C1-H1⋯Cg6	1.00	2.56	3.5235(17)	161	*x* + 1, *y*, *z*
	C5-H5⋯O8	1.00	2.45	3.3003(18)	143	-*x*, -*y*, -*z* + 2
	C6-H6⋯O5	1.00	2.38	3.3666(18)	171	-*x* + 1, -*y*, -*z*+ 2
	C7-H7⋯O8	1.00	2.50	3.2464(18)	132	-*x* + 1, -*y*, -*z*+ 2
	C14-H14⋯O4	0.95	2.38	3.2950(19)	162	*x* + 1, *y*, *z*

Table S2. Interactions linking molecular helices and bilayers in solvates of **12**.

Group I (P2₁/c)	D-H…A	D-H (Å)	H-A (Å)	D-A (Å)	∠D-H…A / α (°)	Symmetry codes
12•CH_3COCH_3	C13-H13⋯F2	0.95	2.64	3.127(3)	113	*x* - 1, -*y* + 1/2, *z* - 1/2
	C14-H14⋯O8	0.95	2.49	3.190(3)	130	-*x* + 2, -*y*, -*z*
	Cg5⋯Cg5			4.0071(16)	0.00(11)	-*x* + 2, -*y* + 1, -*z*
12•CH_3NO_2	C13-H13⋯F2	0.95	2.49	3.224(3)	134	*x* + 1, -*y* + ½, *z* – 1/2
	C14-H14⋯O8	0.95	2.42	3.135(3)	132	-*x* + 1, -*y*, -*z*
	Cg5⋯Cg5			4.4664(13)	0.00(9)	-*x* + 1, -*y* + 1, -*z*
12•CH_3SOCH_3	C13-H13⋯F2	0.95	2.68	3.161(3)	112	*x* – 1, -*y* + 3/2, *z* – 1/2
	C14-H14⋯O8	0.95	2.57	3.238(4)	127	-*x* + 1, -*y* + 2, -*z*
	Cg5⋯Cg5			3.9431(15)	0.00(12)	-*x* + 1, -*y* + 1, -*z*
12•*p*-$C_6H_4(CH_3)_2$	C13-H13⋯F2	0.95	2.56	2.9691(17)	106	*x* – 1, -*y* + ½, *z* – 1/2
	C14-H14⋯O8	0.95	2.59	3.2690(18)	128	-*x*, -*y* + 1, -*z*
	Cg5⋯Cg5			4.0582(9)	0.00(7)	-*x*, -*y*, -*z*
Group I (P2₁/n)						
12•$CHCl_3$	C13-H13⋯O8	0.95	2.49	3.286(4)	141	-*x* + 1, -*y* + 1, -*z*
	C18-H18⋯Cg5	0.95	2.96	3.680(3)	134	*x* – ½, -*y* + 3/2, *z* + 1/2
	Cg5⋯Cg5			3.8357(18)	0.00(13)	-*x* + 1, -*y* + 2, -*z*
	Cg6⋯Cg6			3.8815(19)	0.00(13)	-*x* + 1, -*y* + 1, -*z* + 1
12•CH_2Cl_2	C13-H13⋯O8	0.95	2.42	3.161(3)	135	-*x* + 1, - *y*, – *z*
	C18-H18⋯Cg5	0.95	2.85	3.539(2)	130	-1/2 + *x*, -*y* + 1/2, *z* + ½
	Cg5⋯Cg5			4.1424(12)	0.02(9)	-*x* + 1, -*y* + 1, - *z*
	Cg6⋯Cg6			3.9133(12)	0.02(10)	-*x*+ 1, - *y*, -*z* + 1
12•C_4H_8O	C13-H13⋯O8	0.95	2.53	3.208(3)	128	-*x*, -*y* + 1, -*z*
	C18-H18⋯Cg5	0.95	2.64	3.501(3)	151	*x* – ½, -*y* + 3/2, *z* + 1/2
	Cg5⋯Cg5			3.8958(14)	0.00(11)	-*x*, -*y* + 2, -*z*
	Cg6⋯Cg6			4.2767(14)	0.00(12)	-*x*, -*y* + 1, -*z* + 1
12•CCl_4	C13-H13⋯O8	0.95	2.65	3.492(3)	147	-*x* + 1, -*y* + 1,-*z* + 2
	C18-H18⋯Cg5	0.95	3.00	3.733(3)	135	*x* + 1/2,-*y* + 3/2, *z* -1/2
	Cg5⋯Cg5			3.6536(15)	0.02(11)	-*x* + 1,-*y* + 2,-*z* + 2
	Cg6⋯Cg6			4.5789(17)	0.00(13)	-*x*+ 1, -*y* + 1, -*z* + 1
12•$ClCH_2CH_2Cl$	C3-H3⋯F2	1.00	2.53	3.223(3)	126	*x* – ½, -*y* + 3/2, *z* + 1/2
	C13-H13⋯O8	0.95	2.48	3.144(4)	127	-*x* + 1, -*y* + 1, -*z* + 2
	C19-F2⋯Cg6	1.356(4)	3.666(2)	3.502(3)	72.34(15)	-*x* + 1, -*y* + 1, -*z* + 1
	Cg5⋯Cg5			3.7416(15)	0.00(12)	-*x* + 1, -*y* + 2, -*z* + 2
	Cg6⋯Cg6			3.8460(17)	0.00(14)	-*x* + 1, -*y* + 1, -*z* + 1
Group II (P-1)						
12•C_6H_6	C13-H13⋯O3	0.95	2.50	3.3563(17)	150	-*x* + 2, -*y* + 1, -*z*
	C4-H4⋯Cg5	1.00	2.91	3.8939(15)	166	-*x* + 1, -*y* + 1, -*z*
12•$C_6H_5CH_3$	C13-H13⋯O3	0.95	2.53	3.373(4)	147	-*x* – 1, -*y* + 1, -*z*
	C4-H4⋯Cg5	1.00	2.85	3.827(3)	165	-*x*, -*y* + 1, -*z*
12•*o*-$C_6H_4(CH_3)_2$	C13-H13⋯O3	0.95	2.50	3.3572(18)	151	-*x* + 2, -*y* + 1, -*z* + 2
	C4-H4⋯Cg5	1.00	2.80	3.7642(17)	162	-*x* + 1, -*y* + 1, -*z* + 2

α: Dihedral angle between the phenyl rings

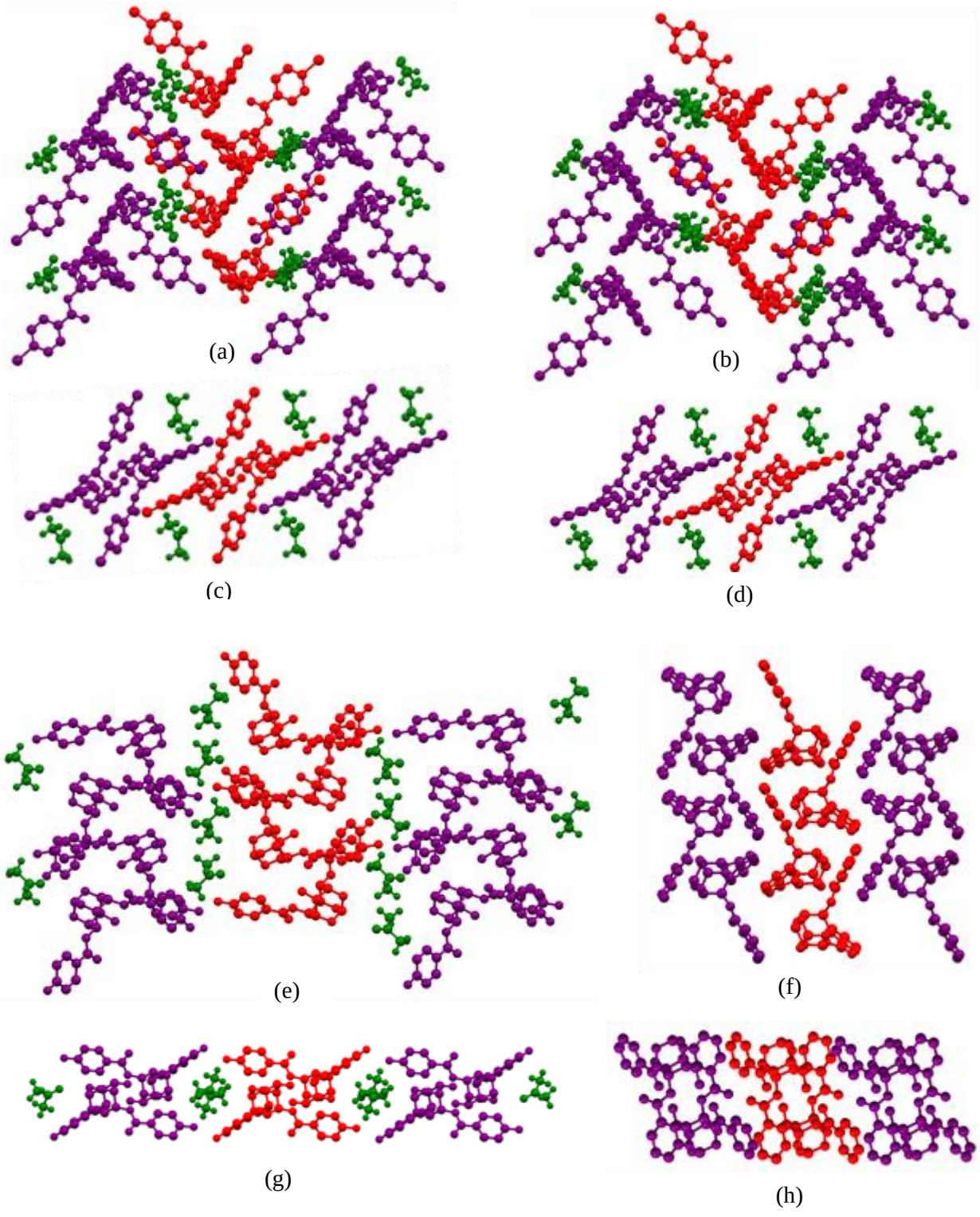

Figure S6. Helices in crystals of (a) **10**•CH_3COCH_3, (b) **11**•CH_3COCH_3, (e)**12**•CH_3COCH_3 and (f) **1**. Enantiomers are denoted as purple and red molecules, solvent acetone is shown in green. (c), (d), (g) and (h) show the top view of the corresponding helices.

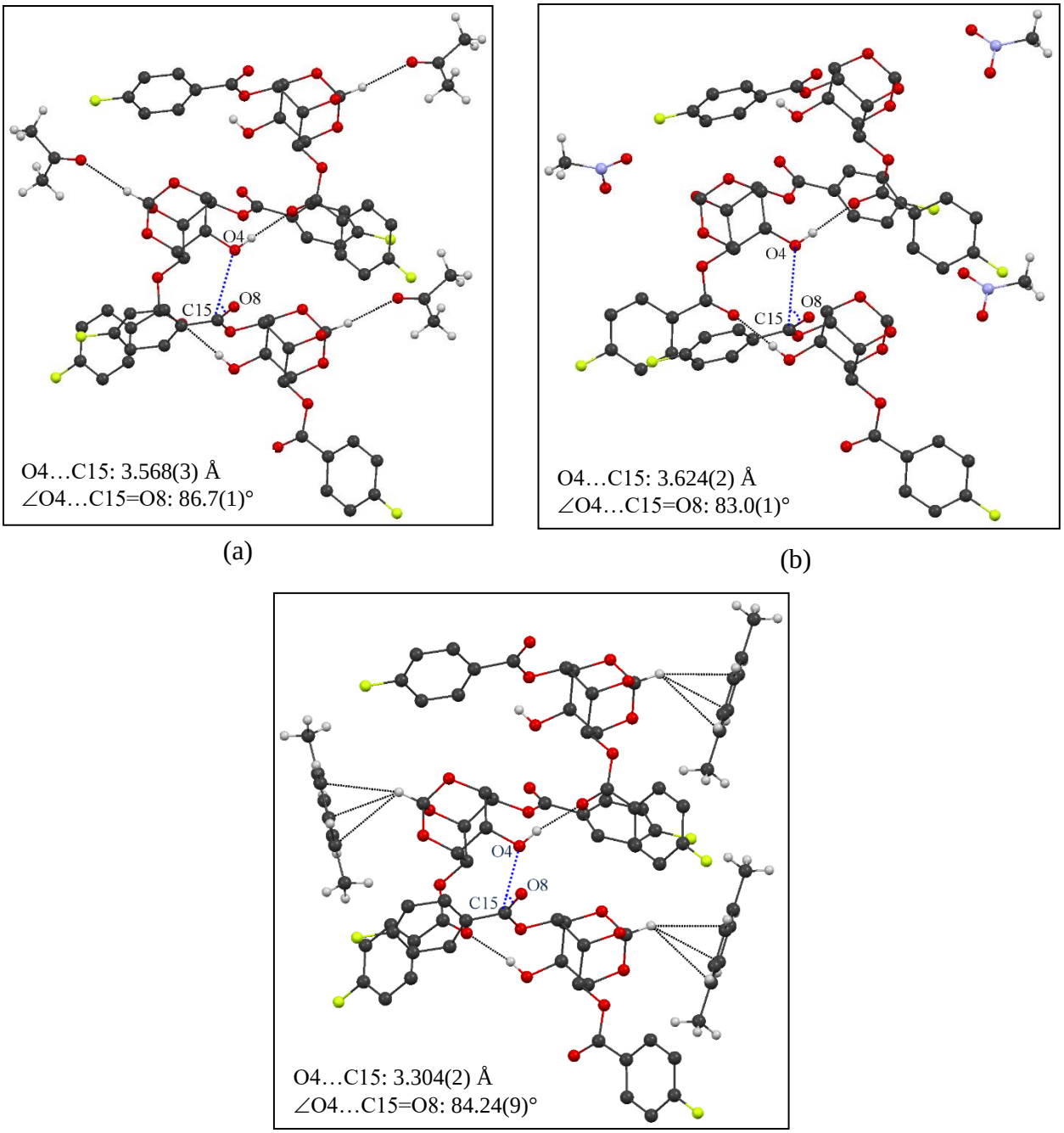

Figure S7. The orientation of the electrophilic and nucleophilic groups in adjacent molecules along the helix in crystals of (a) **12**•CH_3COCH_3, (b) **12**•CH_3NO_2 and (c) **12**•*p*-$C_6H_4(CH_3)_2$.

Host-guest interactions in the solvates

The guest molecules interact with the host molecules mainly *via* C-H···O and C-H···F interactions. The orthoformate H-atom of the host molecule is involved in C-H···O interactions with the oxygen (acetone, THF, and DMSO) atoms of solvent molecules. Significant interactions made by each guest molecule with the host are mentioned below.

12•$CHCl_3$: The H-atom (H22) of the chloroform molecule in 12•$CHCl_3$ forms a short C-H···O contact with the orthoformate bridge oxygen O3 (Fig. S8a, Table S3).

12•CH_3COCH_3: The carbonyl oxygen O9 of acetone in 12•CH_3COCH_3 is involved in short and linear C-H···O interactions with the orthoformate bridge proton (C7-H7) of the host molecules (Figure S8b, Table S3).

12•CH_2Cl_2: The H-atom of the DCM molecule in 12•CH_2Cl_2 interacts with the orthoester oxygen atom O3 through C-H···O contacts (Figure S8c, Table S3).

12•CH_3NO_2: The oxygen atom of CH_3NO_2 molecule in 12•CH_3NO_2 is engaged in C-H…O interactions with the aromatic proton of the axial ester (C17-H17···O9) of the host (Figure S8d, Table S3).

12•C_4H_8O: In **12**•C_4H_8O the guest interacts with the host orthoformate proton through short C7-H7···O9 contacts and the axial ester *via* C17-H17···O9 interactions (Figure S8e, Table S3).

12•CH_3SOCH_3: The guest interacts with host molecules *via* C-H···O(=S) interactions. The oxygen O9 of the DMSO molecule forms C-H···O contacts (Figure S8f, Table S3) with H-atom from the orthoformate group (C7-H7).

12•$ClCH_2CH_2Cl$: The methylene hydrogen (C23′-H23*D*) of dichloroethane is engaged in a short and linear C-H···O interaction with the orthoester oxygen O3 (Table S3).

12•*p*-$C_6H_4(CH_3)_2$: The *p*-xylene solvate **12**•*p*-$C_6H_4(CH_3)_2$ is isostructural with the corresponding solvates of (**10**) and (**11**). The *p*-xylene molecule interacts with the host through weak C-H···O interactions involving aromatic protons (C22-H22) and the orthoester bridge ether oxygen O3.

12•C_6H_6, **12**•$C_6H_5CH_3$ and **12**•*o*-$C_6H_4(CH_3)_2$: In the triclinic solvates **12**•C_6H_6, **12**•$C_6H_5CH_3$ and **12**•*o*-$C_6H_4(CH_3)_2$, the guest occupies the channel between bilayers along the *b*-axis. Benzene, toluene and *o*-xylene molecules interact with the host through weak C-H···π interactions (Figure S8g, S8h, S8i, Table S3). In the case of toluene and *o*-xylene, the guest also engages in C-H···F interactions with the host (Figure S8h, S8i).

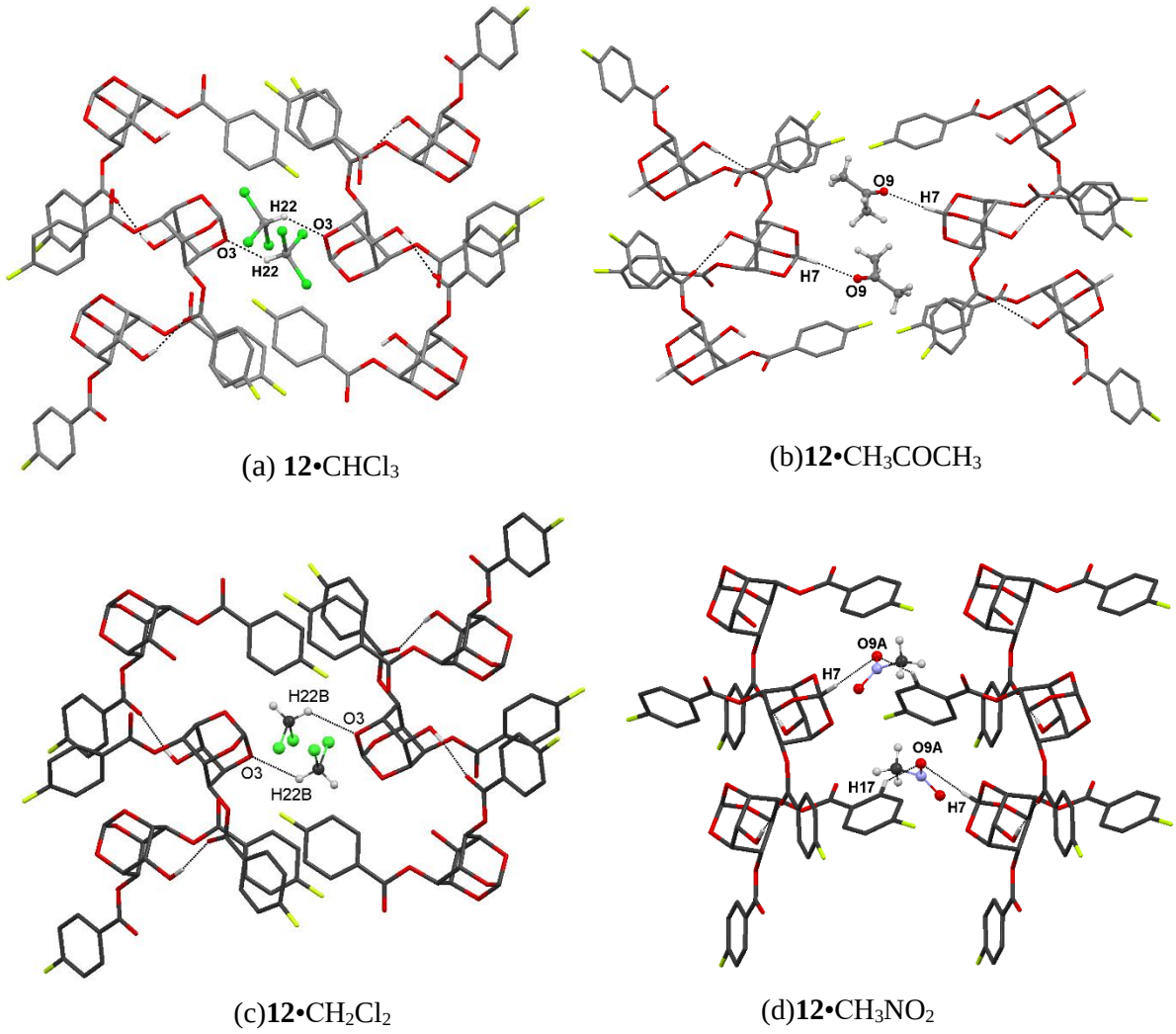

(a) **12**•$CHCl_3$ (b)**12**•CH_3COCH_3

(c)**12**•CH_2Cl_2 (d)**12**•CH_3NO_2

Figure S8. Host guest interactions in solvates of **12**.

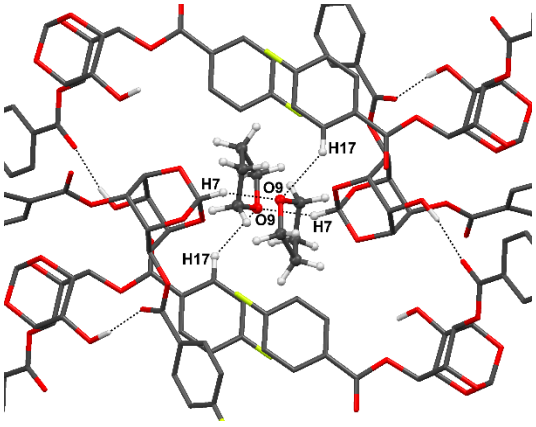

(e)**12**•C_4H_8O

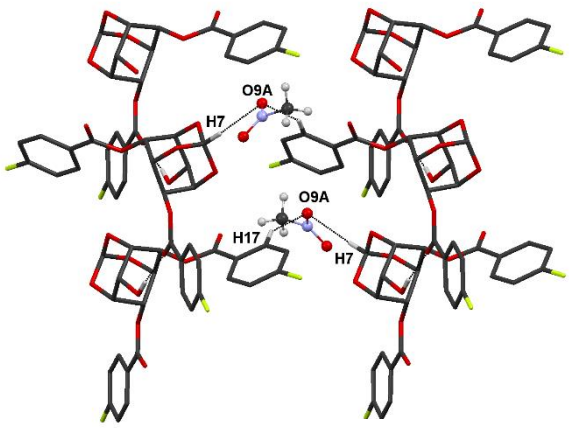

(f)**12**•CH_3SOCH_3

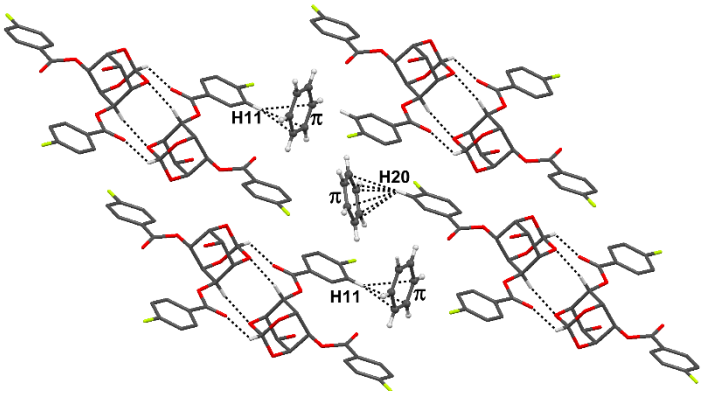

(g)**12**•C_6H_6

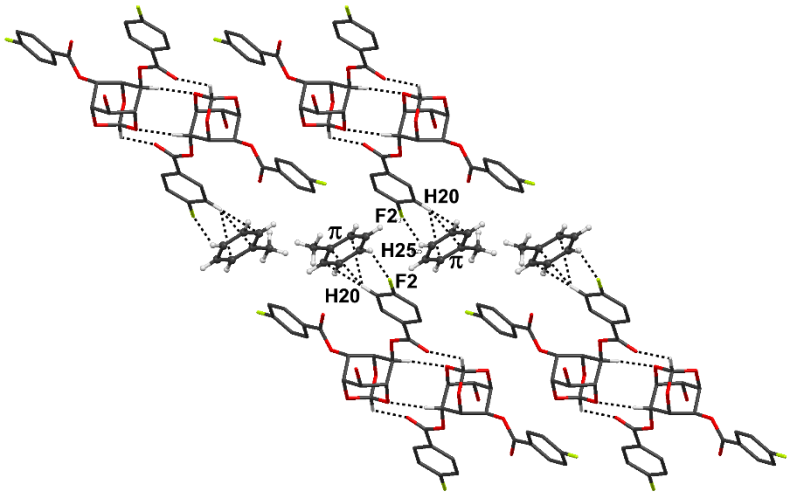

(h)**12**•$C_6H_5CH_3$

Figure S8 (contd.). Host guest interactions in solvates of **12**.

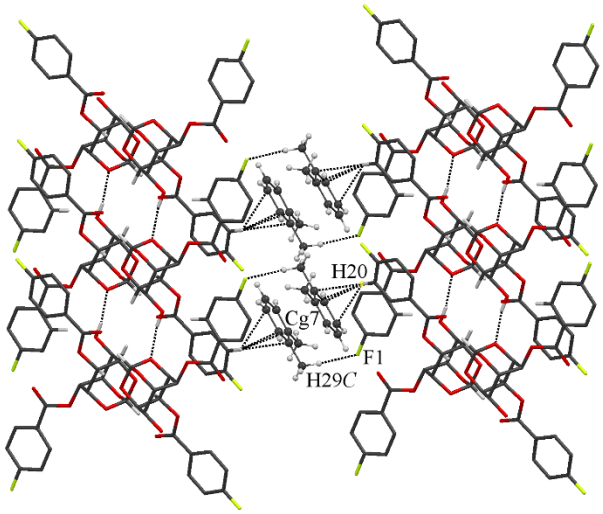

(i) **12**•*o*-$C_6H_4(CH_3)_2$

Figure S8 (contd). Host guest interactions in solvates of **12**.

Table S3. Host guest interactions in solvates of **12**.

Solvate	D-H···A	D-H /Å	H···A /Å	D···A /Å	D-H···A /°	Symmetry Codes
12•$CHCl_3$	C22-H22···O3	1.00	2.48	3.292(4)	138	*–x* + 1, *-y* + 1, *-z*
12•CH_3COCH_3	C7-H7···O9	1.00	2.28	3.281(3)	175	*–x*+1, *-y*+2, *-z*+2
12•CH_2Cl_2	C22B-H22D···O3	0.99	2.48	3.25(3)	134	*x*, *y*, *z*
	C22A-H22B···O3	0.99	2.63	3.36(3)	130	*x*, *y*, *z*
12•CH_3NO_2	C17-H17···O9A	0.95	2.53	3.396(4)	152	*-x*, *-y*, *-z*
	C7-H7···O9A	1.00	2.62	3.618(5)	174	*-x* + 1,*-y* + 1,*-z*
12•C_4H_8O	C7-H7···O9	1.00	2.32	3.266(3)	158	*–x* + 1, *-y* + 1, *-z*
	C17-H17···O9	0.95	2.54	3.254(3)	132	*–x* + 1/2, *y* – 1/2, *-z* + 1/2
12•CCl_4	C14-H14···Cl4	0.95	2.81	3.490(4)	129	*x* -1/2,*-y* + 1/2,*z* + 1/2
12•CH_3SOCH_3	C7-H7···O9	1.00	2.19	3.186(4)	177	*–x*, *-y* + 2, *-z*
12•$ClCH_2CH_2Cl$	C23′-H23*D*···O3	0.99	2.53	3.394(8)	145	*-x* + 1, *-y* + 1, *-z* + 2
12•C_6H_6	C11-H11···Cg11		2.70	3.5352(17)	147	*–x* + 2, *-y*, *-z* + 1
	C20-H20···Cg10		2.81	3.5477(17)	136	*–x* + 1, *-y* + 1, *-z* + 1
	C11-H11···Cg11		2.70	3.5352(17)	147	*x*, *y*, *z*
	C20-H20···Cg10		2.81	3.5477(17)	136	*x* – 1, *y*, *z*
12•$C_6H_5CH_3$	C25-H25···F2	0.95	2.50	3.294(5)	141	*x* – 1, *y*, *z*
	C20-H20···Cg10	0.95	2.70	3.417(4)	132	*x*, *y*, *z*
12•*o*-$C_6H_4(CH_3)_2$	C29-H29*C*···F1	0.98	2.51	3.463(3)	164	*x* - 1, *y*, *z*
	C20-H20···Cg7	0.95	2.63	3.375(3)	136	*–x*, *-y* + 1, *-z* + 1

Table S4. Electrophile-nucleophile geometry in crystals of racemic 2,6-di-*O*-acyl *myo*-inositol orthoformates.

Crystal	El-Nu (d Å) (O4...C15=O8)	El-Nu (∠ °) (O4...C15=O8)	Symmetry codes	Length of helix per turn (Å)
1	3.216(3), 3.249(5)	88.3(1), 89.9(3)	*-x* + 1, *y* + ½, *-z* + ½, *-x* + 2, *y* – ½, *-z* + ½	9.828(4)
2	3.135(4)	87.6(2)	*-x* + ½, *y* – ½, *-z* + ½	9.383(6)
3	3.144(2)	85.6(1)	*-x*, *y* – ½, *-z* + ½	9.465(3)
10•$CHCl_3$	4.054(4)	44.6(1)	*–x* + 3/2, *y* + 1/2, *-z* + 3/2	10.260(2)
10•CH_3COCH_3	4.146(4)	48.5(2)	*–x* + ½, *y* + ½, *-z* + ½	10.205(1)
10•CH_2Cl_2	4.178(4)	65.7(2)	*–x* + 3/2, *y* + ½, *-z* + ½	10.202(2)
10•CH_3NO_2	4.335(4)	46.0(1)	*–x* + 3/2, *y* + 1/2, *-z* + 3/2	10.153(1)
10•$ClCH_2CH_2Cl$	4.242(5)	83.4(2)	*–x* + 1, *y* + ½, *-z* + 3/2	10.010(1)
11•$CHCl_3$	4.170(3)	46.5(1)	*–x* + 3/2, *y* + 1/2, *-z* + 3/2	10.271(1)
11•CH_3COCH_3	4.172(3)	47.5(1)	*–x* + ½, *y* + ½, *-z* + ½	10.221(2)
11•CH_3NO_2	4.334(2)	83.0(1)	*–x* + ½, *y* + ½, *-z* + ½	10.0712(8)
11•$ClCH_2CH_2Cl$	4.208(5)	84.0(3)	*–x* + 2, *y* + 1/2 , *-z* + ½	9.911(3)
11•CH_3CN	3.939(3)	83.4(1)	*–x* + 2, *y* + 1/2 , *-z* + ½	9.86(2)
12•CH_3COCH_3	3.568(3)	86.7(1)	*–x* + 2, *y* + ½, *-z* + 1/2	9.513(3)
12•CH_2Cl_2	4.144(2)	46.0(1)	*–x* + 3/2, *y* + ½, *-z* + ½	10.104(2)
12•CH_3NO_2	3.624(2)	83.0(1)	*–x* + 1, *y* + ½, *-z* + ½	9.618(3)
12•C_4H_8O	4.068(3)	57.7(1)	*–x* + ½, *y* + ½, *-z* + ½	10.202(3)
12•$ClCH_2CH_2Cl$	4.259(3)	64.8(2)	*–x* + 1/2, *y* + 1/2 , *-z* + 3/2	10.052(3)
12•*p*-$C_6H_4(CH_3)_2$	3.304(2)	84.24(9)	*–x*, *y* + ½, *-z* + 1/2	9.362(2)
12•FI	-	-	-	-

Table S5. Summary of crystallographic data for **12**•FI, **15**, **18** and solvates of **12**.

	12•FI	**12**•$CHCl_3$	**12**•CH_3COCH_3	**12**•CH_2Cl_2
Chemical formula	$C_{21}H_{16}F_2O_8$	$C_{21}H_{16}F_2O_8$• $CHCl_3$	$C_{21}H_{16}F_2O_8$• CH_3COCH_3	$C_{21}H_{16}F_2O_8$• CH_2Cl_2
M_r	434.34	553.70	492.41	519.26
Temperature (K)	297(2)	133(2)	133(2)	133(2)
Morphology	Block	Plate	Plate	Plate
Crystal size	0.45 × 0.10 × 0.03	0.30 × 0.14 × 0.05	0.37 × 0.17 × 0.12	0.55 ×0.18× 0.14
Crystal system	Monoclinic	Monoclinic	Monoclinic	Monoclinic
Space group	$P2_1/n$	$P2_1/n$	$P2_1/c$	$P2_1/n$
a (Å)	11.5791(18)	12.869(3)	11.476(2)	12.8215(15)
b (Å)	6.7493(10)	10.168(2)	9.5127(17)	10.1040(12)
c (Å)	24.277(4)	17.234(4)	20.424(4)	17.172(2)
α (°)	90	90	90	90
β (°)	92.685(3)	99.870(4)	90.219(3)	100.146(2)
γ (°)	90	90	90	90
V (Å^3)	1895.2(5)	2221.6(9)	2229.6(7)	2189.8(4)
Z D_{calc} (g cm^{-3})	4 1.522	4 1.655	4 1.467	4 1.575
μ(mm^{-1}) *F(000)*	0.13 896	0.48 1128	0.12 1024	0.36 1064
T_{min} T_{max}	0.876 1.000	0.705 1.000	0.730 1.000	0.869 1.000
h, k, l (min, max)	(-13,13), (-8,8), (-28,28)	(-14,15), (-12,12), (-20,20)	(-12,13), (-11.11), (-22,24)	(-15,13), (-12,10), (-20,20)
Reflns collected	17500	30912	21208	10797
Unique reflns	3316	3487	3917	3865
Observed reflns R_{int}	2201 0.045	3920 0.065	3708 0.049	3636 0.0159
No. of parameters	284	320	343	323
GoF	1.01	1.157	1.11	1.038
$R_1[I > 2\sigma(I)]$	0.040	0.051	0.060	0.0408
$wR_2[I > 2\sigma(I)]$	0.081	0.119	0.167	0.0990
R_1_all data	0.073	0.059	0.062	0.0429
wR_2_all data	0.092	0.124	0.169	0.1007
$\Delta\rho_{max}$, $\Delta\rho_{min}$(e Å^{-3})	0.17, -0.14	0.49, -0.36	0.46, -0.29	0.87, -0.54
CCDC No.	1495458	1495459	1495460	1495461

Table S5 (contd). Summary of crystallographic data for **12**•FI, **15**, **18** and solvates of **12**.

	12•CH_3NO_2	**12**•C_4H_8O	**12**•CCl_4	**12**•CH_3SOCH_3
Chemical formula	$C_{21}H_{16}F_2O_8$• CH_3NO_2	$C_{21}H_{16}F_2O_8$• C_4H_8O	$C_{21}H_{16}F_2O_8$• CCl_4	$C_{21}H_{16}F_2O_8$• CH_3SOCH_3
M_r	495.38	506.44	588.15	512.46
Temperature (K)	133(2)	133(2)	133(2)	133(2)
Morphology	Plate	Plate	Plate	Plate
Crystal size	0.32 ×0.26 ×0.07	0.24 ×0.19 ×0.10	0.47 ×0.18 ×0.11	0.38 ×0.16 ×0.14
Crystal system	Monoclinic	Monoclinic	Monoclinic	Monoclinic
Space group	$P2_1/c$	$P2_1/n$	$P2_1/n$	$P2_1/c$
a (Å)	11.5876(16)	12.6350(14)	12.425(2)	11.5353(10)
b (Å)	9.6180(13)	10.2016(11)	10.3074(16)	9.5572(8)
c (Å)	19.653(3)	17.8698(19)	18.643(3)	20.5755(17)
α (°)	90	90	90	90
β (°)	95.241(2)	101.388(2)	102.994(3)	91.3960(10)
γ (°)	90	90	90	90
V (Å^3)	2181.2(5)	2258.0(4)	2326.5(6)	2267.7(3)
Z	4	4	4	4
D_{calc} (g cm^{-3})	1.509	1.490	1.679	1.501
μ(mm^{-1})	0.13	0.12	0.57	0.21
F(000)	1024	1056	1192	1064
T_{min}	0.831	0.749	0.793	0.702
T_{max}	1.000	1.000	1.000	1.000
h, k, l (min, max)	(-13,13), (-11,9), (-23,19)	(-15,14), (-10,12), (-21,21)	(-14,14), (-12,12), (-19,22)	(-10,13), (-11,11), (-24,24)
Reflns collected	10568	11011	11308	10998
Unique reflns	3837	3970	4085	3984
Observed reflns	3416	3494	3484	3487
R_{int}	0.0165	0.055	0.0398	0.0168
No. of parameters	351	329	366	347
GoF	1.031	0.93	1.03	1.054
$R_1[I > 2\sigma(I)]$	0.0466	0.055	0.048	0.0600
$wR_2[I > 2\sigma(I)]$	0.1225	0.139	0.115	0.1341
R_1_all data	0.0515	0.061	0.056	0.0674
wR_2_all data	0.1267	0.145	0.121	0.1389
$\Delta\rho_{max}$, $\Delta\rho_{min}$(e Å^{-3})	0.89, -0.22	0.39, -0.22	0.52, -0.41	0.59, -0.91
CCDC No.	1495462	1495463	1495464	1495465

Table S5 (contd) Summary of crystallographic data for **12**•FI, **15**, **18** and solvates of **12**.

	12•$C_2H_4Cl_2$	**12**•*p*-$C_6H_4(CH_3)_2$	**12**•C_6H_6	**12**•$C_6H_5CH_3$
Chemical formula	$C_{21}H_{16}F_2O_8$• $C_2H_4Cl_2$	$C_{21}H_{16}F_2O_8$• 0.5*p*-$C_6H_4(CH_3)_2$	$C_{21}H_{16}F_2O_8$• C_6H_6	$C_{21}H_{16}F_2O_8$• $C_6H_5CH_3$
M_r	533.29	487.42	512.44	526.47
Temperature (K)	133(2)	133(2)	133(2)	133(2)
Morphology	Plate	Plate	Block	Block
Crystal size	0.21 ×0.16 ×0.10	0.43 ×0.22 ×0.14	0.25 ×0.24 ×0.12	0.26 ×0.08× 0.07
Crystal system	Monoclinic	Monoclinic	Triclinic	Triclinic
Space group	$P2_1/n$	$P2_1/c$	P-1	P-1
a (Å)	13.3061(12)	11.2679(13)	6.7449(4)	6.8762(8)
b (Å)	10.0518(9)	9.3620(11)	11.5178(8)	11.6387(13)
c (Å)	17.0729(15)	20.990(2)	15.5671(10)	15.4094(18)
α (°)	90	90	77.7590(10)	81.028(2)
β (°)	98.5050(10)	93.908(2)	88.9710(10)	89.700(2)
γ (°)	90	90	88.3540(10)	87.389(2)
V (Å^3)	2258.4(3)	2209.1(4)	1181.28(13)	1216.9(2)
Z D_{calc} (g cm^{-3})	4 1.568	4 1.466	2 1.441	2 1.437
μ(mm^{-1}) *F(000)*	0.35 1096	0.12 1012	0.12 532	0.12 548
T_{min} T_{max}	0.845 1.000	0.811 1.000	0.867 1.000	0.626 1.000
h, *k*, *l* (min, max)	(-15,15), (-11,11), (-20,20)	(-13,12), (-11,10), (-24,24)	(-8,8), (-13,13), (-18,18)	(-8,8), (-13,13), (-18,18)
Reflns collected	15936	10818	11465	10385
Unique reflns	3969	3870	4141	4257
Observed reflns R_{int}	3685 0.026	3524 0.018	3937 0.016	3648 0.032
No. of parameters	348	321	338	348
GoF	1.07	1.03	1.11	1.21
$R_1[I > 2\sigma(I)]$	0.054	0.035	0.038	0.069
$wR_2[I > 2\sigma(I)]$	0.139	0.087	0.095	0.155
R_1_all data	0.058	0.038	0.039	0.080
wR_2_all data	0.141	0.089	0.097	0.160
$\Delta\rho_{max}$, $\Delta\rho_{min}$(e Å^{-3})	0.37, -0.43	0.30, -0.21	0.31, -0.28	0.48, -0.24
CCDC No.	1495466	1495467	1495468	1495469

Table S5 (contd) Summary of crystallographic data for **12**•FI, **15**, **18** and solvates of **12**.

	12•*o*-$C_6H_4(CH_3)_2$	**15**	**18**
Chemical formula	$C_{21}H_{16}F_2O_8$• *o*-$C_6H_4(CH_3)_2$	$C_{28}H_{19}F_3O_9$	$C_{14}H_{13}FO_7$
M_r	540.50	556.43	312.24
Temperature (K)	133(2)	297(2)	297(2)
Morphology	Block	Plate	Plate
Crystal size	0.25 ×0.19 ×0.14	0.30 ×0.20 ×0.07	0.49 × 0.35× 0.11
Crystal system	Triclinic	Monoclinic	Orthorhombic
Space group	*P*-1	$P2_1/n$	*Pbcn*
a (Å)	6.7954(10)	14.060(3)	19.047(4)
b (Å)	11.6754(17)	10.592(3)	10.1896(19)
c (Å)	16.069(2)	17.702(4)	13.462(3)
α (°)	95.891(2)	90	90
β (°)	90.066(2)	110.548(4)	90
γ (°)	91.056(2)	90	90
V (Å^3)	1267.9(3)	2468.4(10)	2612.8(9)
Z D_{calc} (g cm^{-3})	2 1.416	4 1.497	8 1.588
μ(mm^{-1}) *F(000)*	0.11 564	0.13 1144	0.14 1296
T_{min} T_{max}	0.868 1.000	0.697 1.000	0.814 1.000
h, *k*, *l* (min, max)	(-8,8), (-13,13), (-19,19)	(-16,11), (-12,12), (-21,21)	(-22,17), (-12,11), (-16,15)
Reflns collected	12240	12125	12331
Unique reflns	4431	4342	2297
Observed reflns R_{int}	4144 0.022	3400 0.022	1938 0.028
No. of parameters	433	361	207
GoF	0.89	1.04	1.05
$R_1[I > 2\sigma(I)]$	0.039	0.042	0.036
$wR_2[I > 2\sigma(I)]$	0.108	0.095	0.087
R_1_all data	0.041	0.057	0.043
wR_2_all data	0.111	0.102	0.093
$\Delta\rho_{max}$, $\Delta\rho_{min}$(e Å^{-3})	0.25, -0.18	0.23, -0.20	0.16, -0.25
CCDC No.	1495470	1495471	1495472